Discussion

I have discussed the attempts made to explain the optical and infrared line and continuum radiation from Be stars. In the case of optical line emission, the flux produced by the HII region formed by absorption of the Lyman continuum of the Be star is not enough to explain the observed flux; additional ionizing radiation is needed. Alternatively, there could be heating processes occurring in the gas envelope, for example heating produced by shocks, which could result in the needed ionized gas. These processes need to be explored. The optical continuum is adequately explained by the emission from HII regions produced either by the radiation from the Be star or by radiation produced by an accreting compact binary companion. However, excess optical radiation produced in some Be stars, without accompanying H_α emission, is not explained by the emission from the HII regions and remains unaccounted for.

The infrared line emission from Be stars seems to arise in the cooler regions of the gas envelope outside the HII region; but only the CaII triplet emission is accounted for quantitatively. The location of and the processes leading to the emission of the other infrared lines need to be explored. The infrared continuum excess was suggested to be from the ionized regions due to the free–free and free–bound processes. However, the H_α emission implied by this is not observed. In addition, the Lyman continuum from Be stars of later spectral types is not adequate to produce the requisite ionization. Thus the source of the infrared continuum excess from Be stars remains unidentified.

1. Struve, O., *Astrophys. J.*, 1931, **73**, 94.
2. Apparao, K. M. V., Anita, H. M. and Chitre, S. M., *Astron. Astrophys.*, 1987, **177**, 198.
3. Baade, D., *Physics of Be Stars* (eds. Slettebak, A. and Snow, T. P.), Cambridge University Press, England, 1987, p. 361.
4. Harmanec, P., IAU Colloquium no. 92, 1987, p. 339
5. Harmanec, P. and Kriz, S., IAU Colloquium no. 70, 1987, p. 385.
6. Apparao, K. M. V., *Be Stars News Letter*, 1991a, **23**, 11.
7. Apparao, K. M. V. and Tarafdar, S. P., *Astrophys. J.*, 1987, **322**, 976.
8. Kurucz, R. L., *Astrophys. J. (suppl.)*, 1979, **40**, 1.
9. van den Heuvel, E. P. J. and Rappaport, S., IAU Colloquium no. 82, 1987, p. 291.
10. Apparao, K. M. V., *Astrophys. J.*, 1991, **376**, 256.
11. Apparao, K. M. V. and Tarafdar, S. P., *Astron. Astrophys.*, 1991, (submitted).
12. Kallman, T. R. and McCray, R., *Astrophys. J.*, (suppl.) 1982, **50**, 263.
13. Doazan, V. *et al.*, *Astron. Astrophys.*, 1983, **128**, 111.
14. Bartolini, C. *et al.*, IAU Circ. no. 3167, 1977.
15. Rossiger, S., *Dis Sterne*, 1979, **2**, 76.
16. Kriss, G. A., *et al.*, *Astrophys. J.*, 1983, **266**, 806.
17. Apparao, K. M. V. and Tarafdar, S. P., *Astron. Astrophys.*, 1988, **192**, 255
18. Lamers, H. G. J. L. M., IAU Colloquium no. 92,1987, p. 219.
19. Apparao, K. M. V. and Tarafdar, S. P., *Be Sar News Lett.*, 1991b, **24**, 12.
20. Woolf, N. J. *et al.*, *Astron. Astrophys.*, 1970, **9**, 25.
21. Gehrz, R. D. *et al.*, *Astrophys. J.*, 1974, **191**, 675.
22. Ashok, N. M. *et al.*, *Mon. Not. R. Astron. Soc.*, 1984, **211**, 471.
23. Waters, L. B. F. M., *Astron. Astrophys.*, 1986, **162** 121.
24. Waters, L. B. F. M. *et al.*, *Astron. Astrophys.*, 198, **185**, 121.
25. Thompson, R. I., *Astrophys. J.*, 1984, **283**, 165.

Search for dark-matter particles

R. Cowsik

Tata Institute of Fundamental Research, Bombay 400005, India, and McDonnell Center for Space Sciences, Washington Univrsity, St Louis, MO 63130, USA

Experiments performed over the last two years have been very successful in drastically reducing the number of viable elementary particles that could possibly constitute the dark matter that dominates the large-scale gravitational dynamics of astronomical systems. The candidates that survive are the light neutrinos, the axion, and a supersymmetric particle with carefully chosen parameters called the neutralino. Baryonic dark matter, which might contribute not insignificantly over small scales, is perhaps present in the form of brown dwarfs, and a search for these is under way. In this article I first review the astrophysical studies which bear on the density and the phase-space structure of the dark-matter particles; then discuss the implications of the various direct and indirect searches for these particles; and, finally, point out alternative suggestions for the candidates and directions for further searches.

The fascination and the challenge of the search for the constituents of dark matter stem from the connection it bears with astronomy, astrophysics and cosmology on the one hand and with nuclear and particle physics on the other. Dark-matter particles are the only relicts that still survive from the epochs prior to the primordial

helium synthesis which took place at about 400 sec after the big bang. Also, along with the solar neutrinos, they constitute one of the few easily accessible probes of the physics beyond the standard model for the elementary particles. I start this review with a brief presentation of the astrophysical abservations that yield the density distribution and the phase-space structure of dark matter, and go on to indicate the distinguishing features of the three categories of candidates for dark matter, designated baryonic, cold and hot. I then analyse the various experimental searches for these candidates, which can be classified under three heads: 'cosmic-ray type', 'indirect' and 'direct'. This analysis leads us to the conclusion that the searches carried out to date effectively rule out the majority of the candidates, leaving the three light neutrinos, the axion, and perhaps a specially constructed, lightest super-symmetric particle as the possible constituents. I suggest possible methods for searching for these particles.

The subject of dark matter in the universe has a fascinating history. In the year 1933 Zwicky[1] obtained the first clue to the existence of dark matter. His analysis was in two steps; first he noted that the dispersion in the line-of-sight velocities of the galaxies in the Coma cluster was about 700 km sec^{-1}, which allowed the mass of the cluster to be determined by the virial relationship

$$M_d \approx \langle v^2 \rangle R/G. \tag{1}$$

Second, the masses of nearby spiral galaxies were estimated by balancing the gravitational force on the stars with the centrifugal force in

$$m_g \approx v_c^2 r_H/G, \tag{2}$$

where v_c is the rotational velocity of stars at the outer edges of the visible galaxy, say at the Holmberg radius, r_H. Now, assuming that the galaxies in Coma are statistically similar to the nearby spirals he estimated the total luminous mass of the cluster as

$$M_l \approx \sum_i m_{gi}, \tag{3}$$

and noted the very interesting fact that

$$M_l \ll M_d \approx 8 M_l. \tag{4}$$

This method was progressively improved upon, and in 1972 Rood *et al.*[2] measured the velocities of several hundred of the galaxies in the Coma cluster to obtain unequivocal evidence for this excess in the dynamical mass, which is called the 'virial discrepancy'.

At this time I had the good fortune to listen to a fine seminar by King on his observations and proposed, along with McClelland[3,4], the hypothesis that weakly interacting particles left over from the big bang, such as the neutrinos, could, if they had a rest mass of even a few eV, form a cloud of invisible gravitating matter around the cluster. The idea was that, since one expects on the average about 110 neutrinos per cubic centimetre in the universe today, compared with a baryonic density of about 10^{-7} cm^{-3}, even with a few eV rest mass, they would dominate the universe gravitationally in the nonrelativistic era and would have, through their mutual interaction, triggered formation of the galaxies. Extensive work done during the late seventies brought out the full import of this suggestion. The density inhomogeneities in such weakly interacting background could grow, without causing undue fluctuations in the microwave background, thus aiding the formation of galaxies, and such particles could indeed contribute the closure density ($\Omega = 1$) without producing excess helium or lithium during the primordial nucleosynthesis. There are several excellent reviews that discuss the variety of observations and theoretical studies pertaining to dark matter in the universe[5]. I now proceed to detail the developments that are relevant to the detection of dark-matter particles.

Density and distribution of dark matter

In the framework of Friedman–Robertson–Walker cosmologies we can define a critical density ρ_c, which separates universes that expand indefinitely ($\rho < \rho_c$) from those that recollapse ($\rho > \rho_c$). In standard notation,

$$\rho_c = \frac{3H_0^2}{8\pi G} \approx 1.9 \times 10^{-29} h^2 \text{ g cm}^{-3}$$
$$\approx 1.05 \times 10^4 h^2 \text{ eV cm}^{-3}, \tag{5}$$
$$\Omega = \rho/\rho_c.$$

The flat Einstein–de Sitter model with $\Omega = 1$ is preferred on the basis of theoretical ideas of 'inflation' because such a value of Ω is independent of epoch and, more importantly, because it provides adequate time for the formation of large-scale structures such as galaxies and clusters of galaxies.

A variety of different methods are adopted in the determination of the contribution to Ω of matter distributed on various scales:

(i) By restricting oneself to bright regions of the galaxy[6], the measured value of the rotation velocity V_c yields the luminous mass of the galaxy (see equation 2); from galaxy counts one gets the number density of galaxies, and the product yields

$$\Omega_{lum} \leq 0.01. \tag{6}$$

(ii) The pioneering efforts of Rubin *et al.*[7] have yielded rotation curves up to very large galactocentric distances, often measured in the 21-cm radio band. Some of these observations are reproduced in Figures 1 and 2. These curves show 'nearly constant velocities

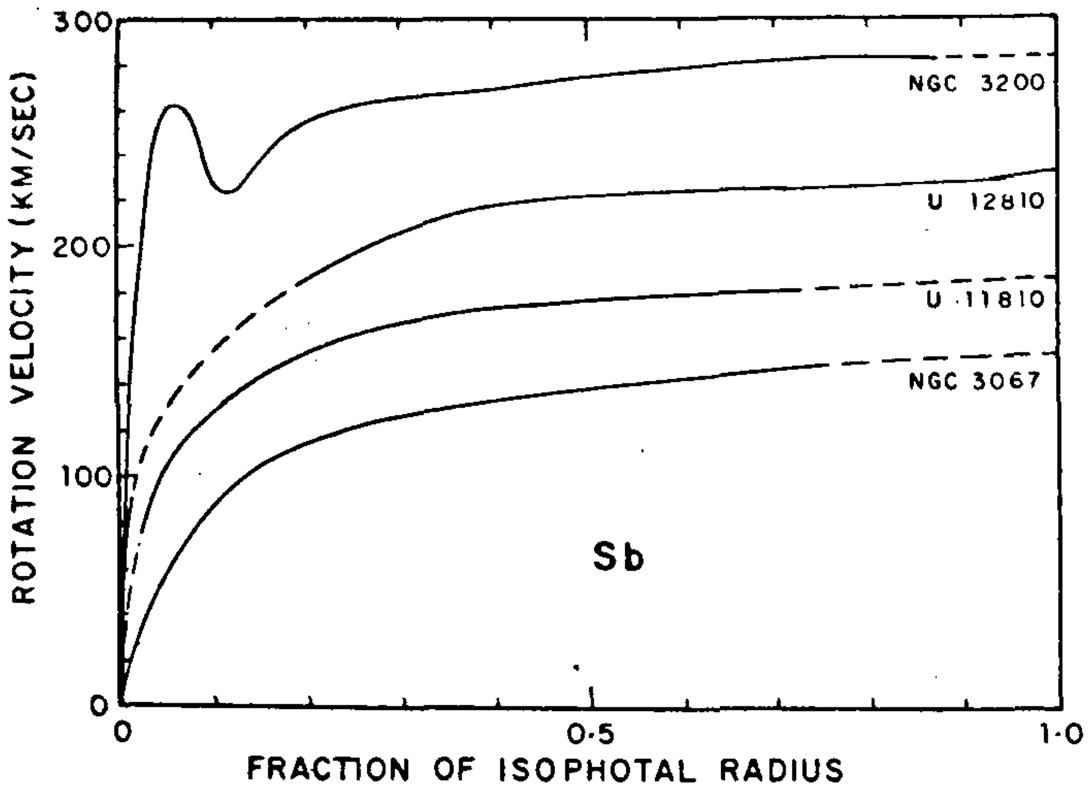

Figure 1. Optical rotation curves of spiral galaxies, arranged in order of increasing luminosity, after Rubin *et al.*[7]

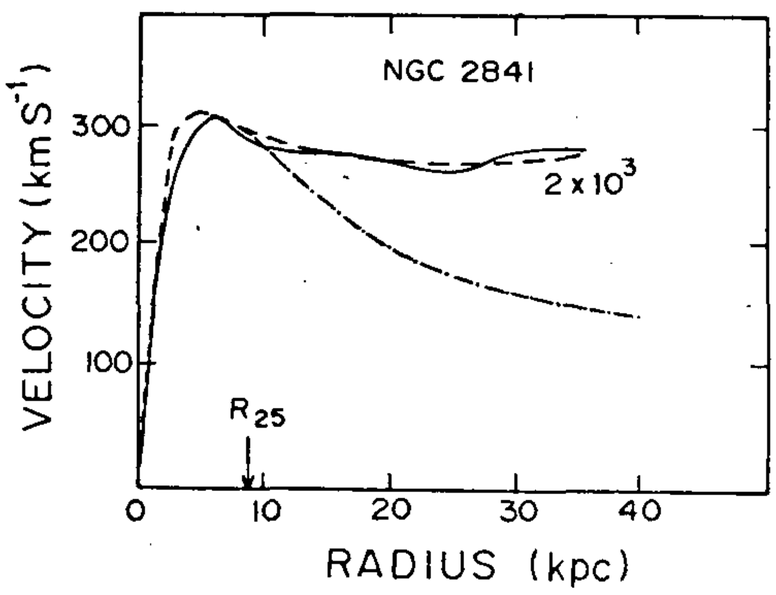

Figure 2. Rotation curve measured using the HI emission at 21 cm by Bosma[7]. The chain-dotted line indicates the rotation curve expected on the basis of luminous matter alone (see Figure 3).

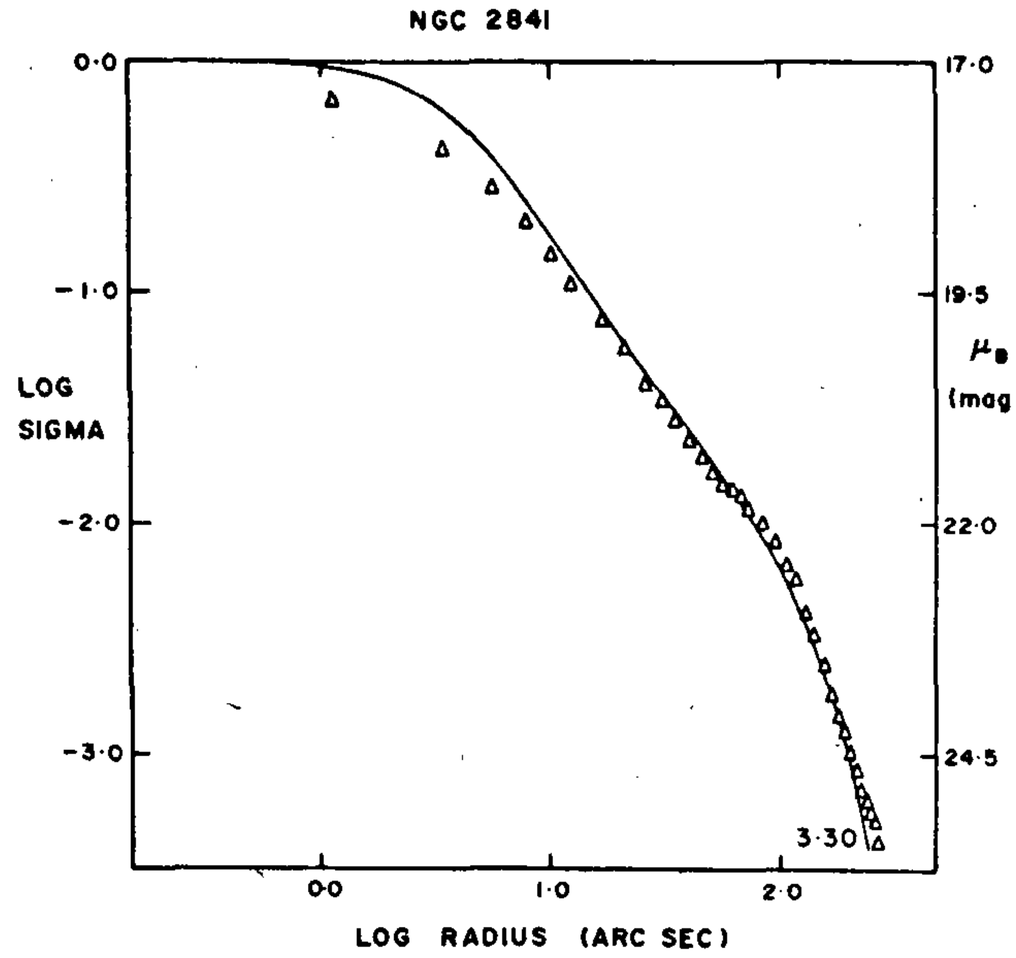

Figure 3. Surface luminosity profile of NBC 2841 measured Boroson[6].

and that significant mass at large ω are the rule'. Figure 3, a typical profile of the luminosity, shows a rapid cut-off in the density of visible matter with distance. The mass contained within a radius ω converges rapidly so that, far beyond the core, the rotation curve should decline as $\approx\omega^{-1/2}$, contrary to the observations. Massive halos of dark matter surrounding the galaxies could provide the requisite gravitational force to balance the centrifugal forces implied by the rotation curves. These studies lead to

$$\Omega_{\text{Halo}} \geq 0.1. \tag{7}$$

If indeed the total mass within some radius were to have converged, then the rotation velocities beyond this radius would have declined in the Keplerian fashion, $\sim\omega^{-1/2}$. It is safe to say that, as yet, there is no observation of any galaxy that shows such a cut-off, and hence the lower limit in equation 7.

(iii) Estimates of the virial masses of clusters following the Zwicky method yield

$$\Omega_{\text{cluster}} \approx 0.1\text{–}0.3. \tag{8}$$

Again this value of Ω_{cluster} pertains only to the m contained within the radius of the visible cluster. Fig 4 shows the mean distribution of galaxies in clust and the requisite background of dark matter needed explain the virial discrepancy. Should the density invisible matter fall as r^{-2}, as expected for isothermal sphere[8], then the total contribution integ ted up to about 50 megaparsecs (Mpc) from the cent of clusters could yield $\Omega \sim 1$.

(iv) The 'peculiar velocities' of the galaxies with resp

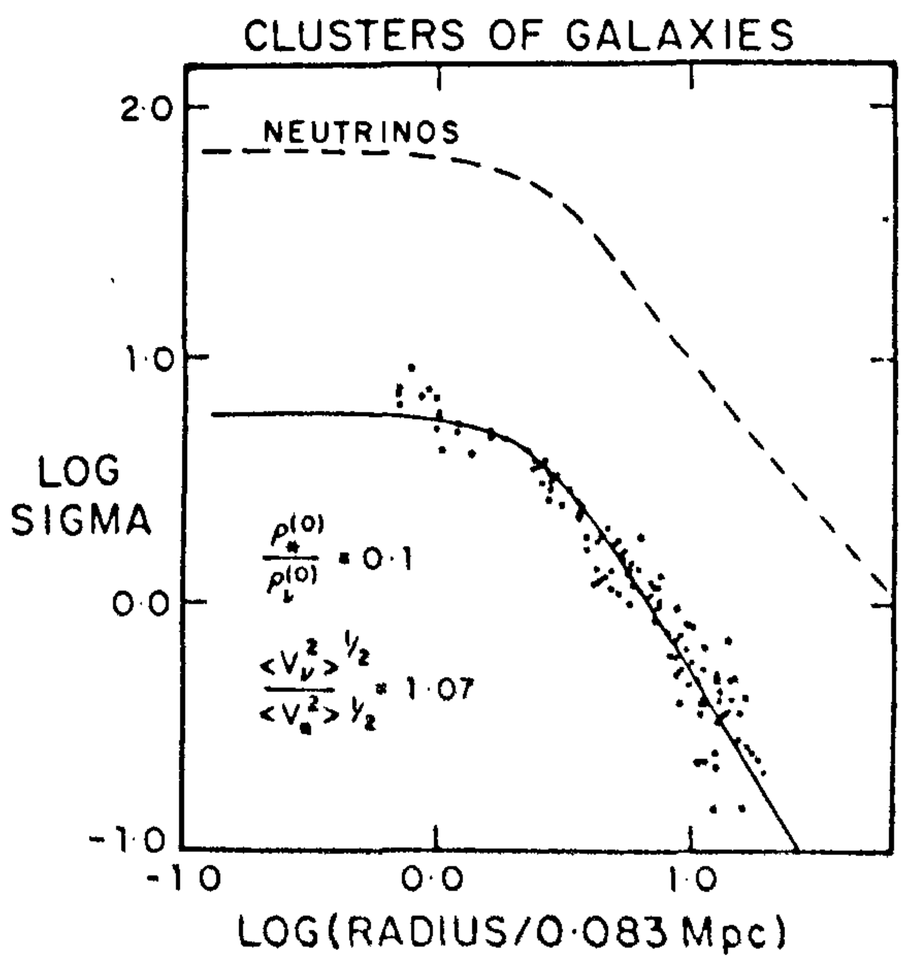

Figure 4. Profiles of surface density of 15 clusters of galaxies (dc superposed on theoretical profile (solid line) and the distribution dark matter (dashed line labelled 'neutrinos') (ref. 8).

to the Hubble flow are sensitive to fluctuations in the densities and to the value of Ω according to the equation

$$\delta v(r) = -\Omega^{0.6}\frac{H_0}{4\pi}\int \delta\rho(r')(r-r')\frac{d^3r'}{|r-r'|^3} \sim \Omega^{0.6} h_0 \lambda \left(\frac{\delta\rho}{\rho}\right)_\lambda, \quad (9)$$

where the approximate relation follows when perturbations on a single scale λ are assumed to dominate. If we further assume that bright galaxies trace the mass, with a possible biasing factor, b, such that

$$\frac{\delta\rho}{\rho} \approx b^{-1}\left(\frac{\delta n_g}{n_g}\right);\ b \sim 1\text{–}3, \quad (10)$$

then the observed distribution of galaxies in the IRAS catalogue yields

$$\Omega = \{(1 \pm 0.3)b\}^{1/0.6} \approx 1. \quad (11)$$

(v) The geometry of the universe is an indicator of its mean density. The volume of the universe contained in a solid angle $d\omega$ in a redshift interval between z and $z + dz$ is sensitive to the value of Ω. It is customary to define q_0 as

$$q_0 \equiv -\frac{\ddot{R}}{H_0^2} = \Omega\left(1 + \frac{3p}{\rho}\right)/2 = \Omega/2. \quad (12)$$

In terms of this q_0 the volume element is

$$\frac{dV}{d\omega dz} = \frac{[zq_0 + (q_0 - 1)((2q_0 z + 1)^{1/2} - 1)]^2}{H_0^3(1+z)^3 q_0^4 [1 - 2q_0 + 2q_0(1+z)^{1/2}]}. \quad (13)$$

If, for example, galaxies are uniformly distributed in z then their number in the interval dz at z will be proportional to the above volume. Thus, by counting their number as a function of z, $q_0 = \Omega/2$ could be determined. The pioneering, yet preliminary efforts of Loh and Spiller[9] with about 1000 galaxies distributed up to $z = 0.75$ yield the result

$$\Omega = 0.9^{+0.7}_{-0.5} \quad (14)$$

Table 1 summarizes these determinations of Ω, and Figure 5 shows the dynamical masses of various systems with respect to their effective radii. There is a general trend, which indicates that the density of dark matter in most systems is nearly constant:

$$10^{-26}\ \mathrm{g\,cm^{-2}} < \rho_{DM} < 10^{-25}\ \mathrm{g\,cm^{-2}}. \quad (15)$$

Table 1. Various determinations of $\Omega \equiv \rho/\rho_c$.

Luminous parts of galaxies	≤ 0.01
Primordial nucleosynthesis	0.04–0.1 ($H_0 = 50$)
Halos of galaxies	≥ 0.1
Clusters of galaxies	~ 0.2–0.3
with isothermal extension	~ 1.0
Peculiar motions	~ 1.0
Galaxy counts up to $z = 0.75$	$0.9^{+0.7}_{-0.5}$

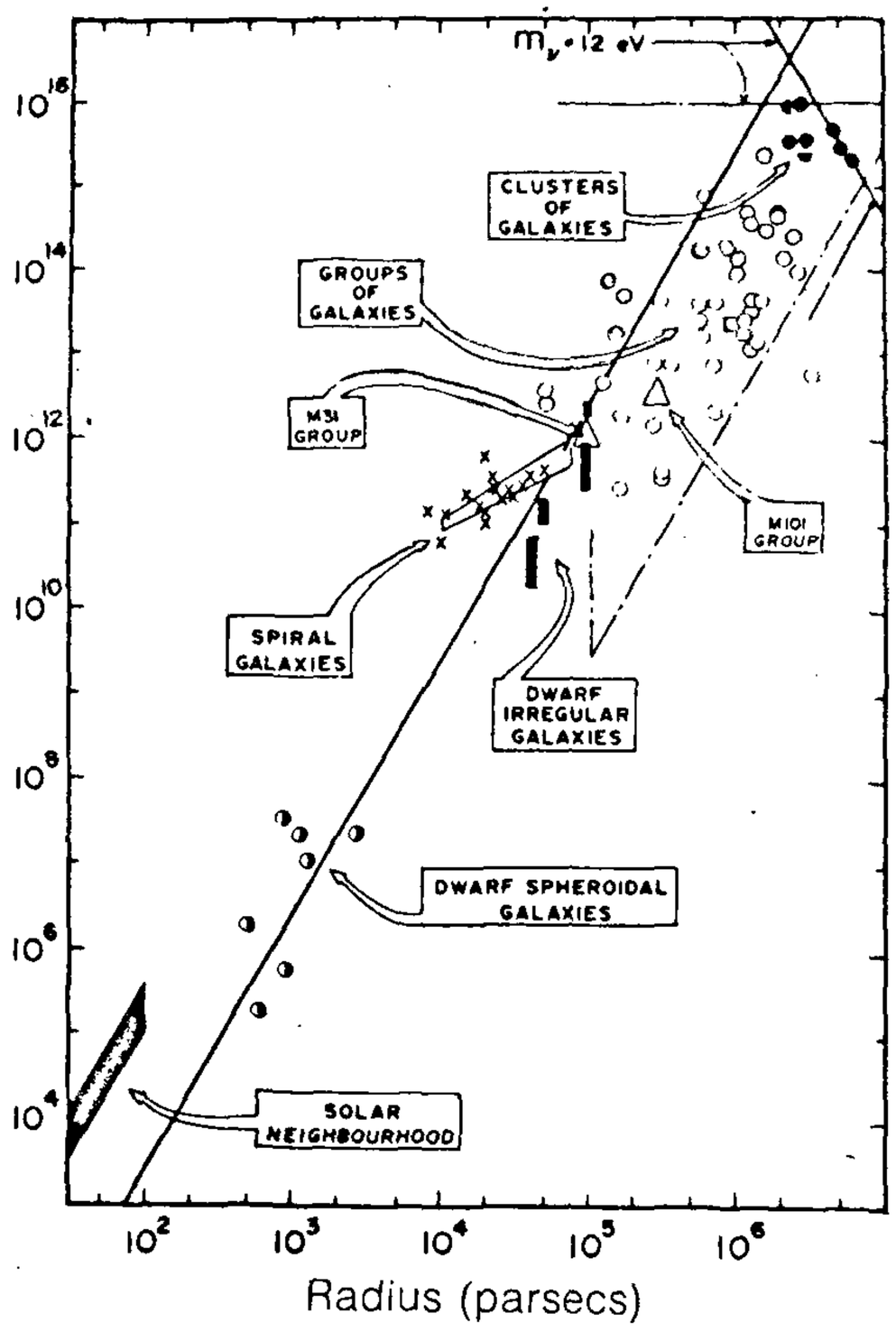

Figure 5. Dynamical masses of various astronomical systems plotted against their effective radii to show their correlation[8].

Dark matter in our galaxy

Estimate of density in solar neighbourhood

An understanding of the related astrophysics is necessary for design and interpretation of experimental searches for dark-matter particles. As with the external galaxies we start with the rotation curve, which is well measured inside the solar circle of galactocentric radius ~ 8.5 kpc, from observations of the emission from HI and CO in the radio and millimetre regions respectively. This is shown in Figure 6. The observations outside the solar circle are more difficult and are even controversial as we are not able to observe the emission at the tangent to the circles about the galactic centre at which the longitudinal first-order Doppler effect is maximal; also the density of visible matter is a rapidly decreasing function of the radius (see Figure 7). We can, however, gain some insight from the observations of companions to our galaxy, such as the globular clusters, the dwarf spheroidals, etc.

The analysis proceeds by trying to estimate the total

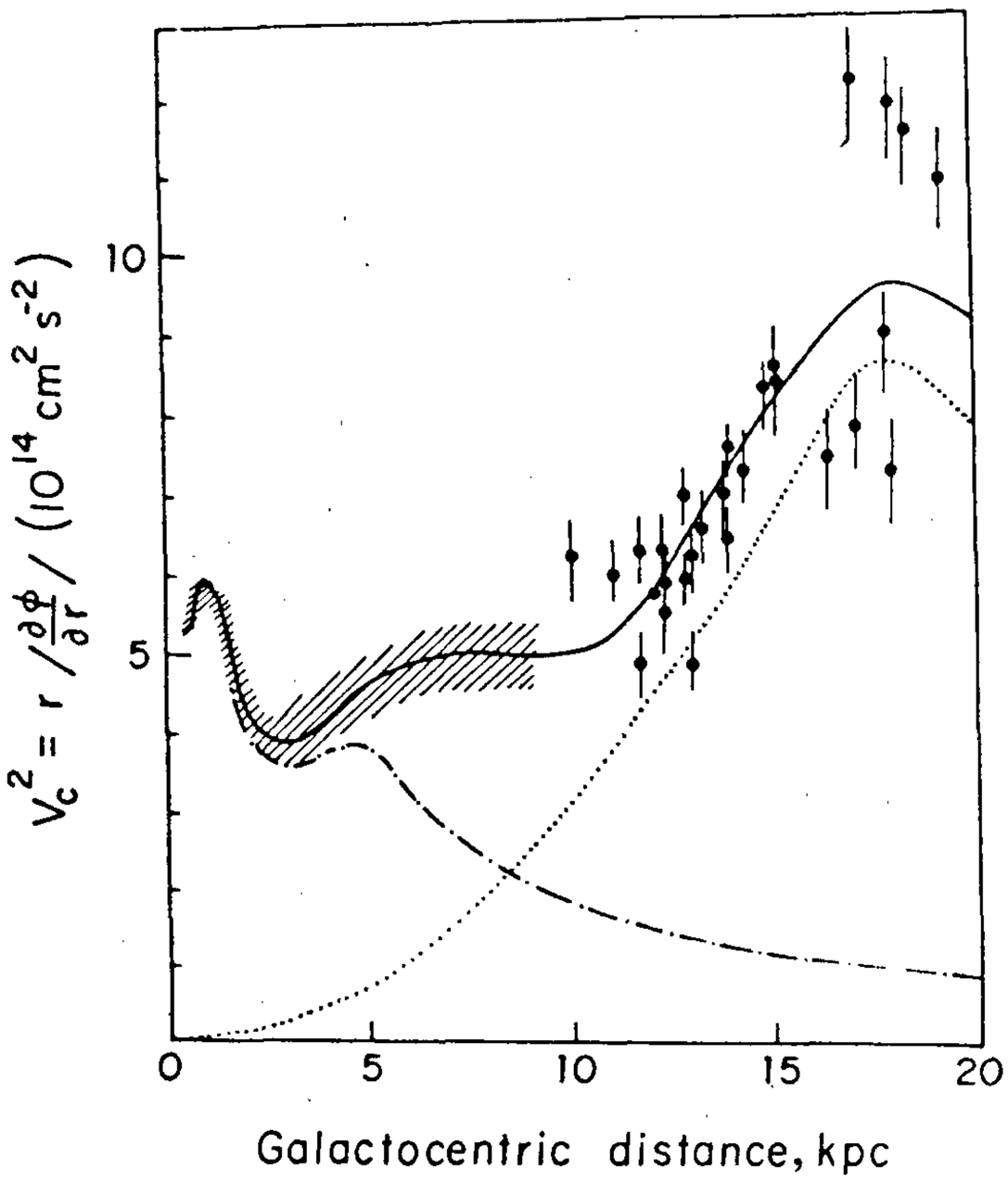

Figure 6. The square of the rotation velocity, V_c^2, in our galaxy plotted against galactocentric distance. The chain-dotted curve is the contribution of visible matter and the dotted curve is that due to dark matter whose distribution is approximated by a modified Hubble profile.

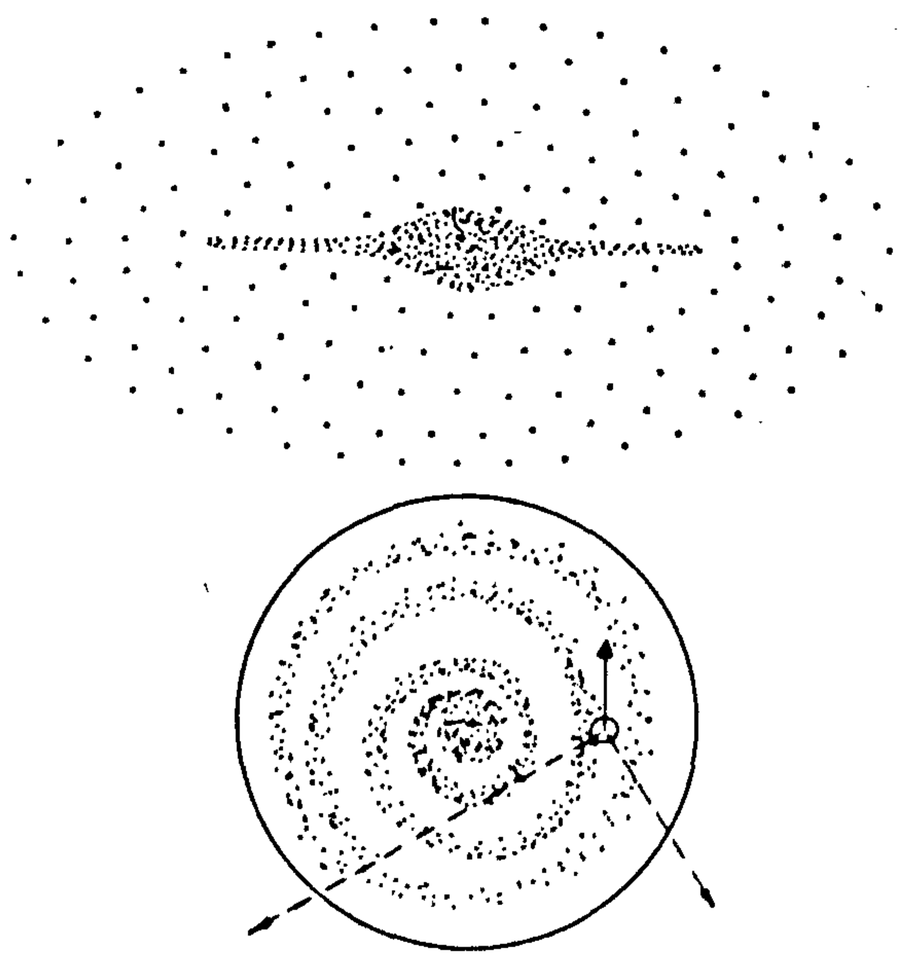

Figure 7. Schematic representation of our galaxy; the upper panel shows an extended spheroidal halo and the lower panel indicates the difficulty of measurement of rotation velocities outside the solar circle.

mass density in the solar neighbourhood ρ_m. Following Oort[10] and Bahcall[11] we write

$$\nabla^2\phi = 4\pi G\rho_m, \tag{16}$$

which, with the assumption of axial symmetry, takes the form

$$\frac{\partial^2\phi}{\partial z^2} + \frac{1}{\omega}\frac{\partial}{\partial\omega}\left[\omega\frac{\partial\phi}{\partial\omega}\right] = 4\pi G\rho_m. \tag{17}$$

Oort argued that $d\phi/d\omega$ was negligible for a thin disc-like system such as our galaxy so that the radial part of the Laplacian could be dropped from the above equation. But the distribution of dark matter about our galaxy could be in the form of an extended halo. Can we then drop the radial term? To ascertain the conditions under which the radial term can be neglected, note that the term within brackets in equation 17 is

$$\omega\frac{\partial\phi}{\partial\omega} = V_c^2. \tag{18}$$

Since, as seen in Figure 6, the rotation velocity $V_c(\omega)$ near the solar circle is nearly constant, its derivative becomes very small near the solar circle.

$$\left|\frac{\partial}{\partial\omega}\left(\omega\frac{\partial\phi}{\partial\omega}\right)\right|_{\omega=\omega_0} = \left|\frac{\partial V_c^2}{\partial\omega}\right|_{\omega=\omega_0} \sim 0. \tag{19}$$

Now the number density of any particular type of star has a distribution in z that is controlled by the Jeans equation:

$$\frac{1}{\nu}\frac{\partial}{\partial z}(\nu\langle v_z^2\rangle) = -\frac{\partial\phi}{\partial z}. \tag{20}$$

In view of equation 17 (without the ω term) this becomes

$$\frac{d}{dz}\left\{\frac{1}{\nu}\frac{d}{dz}(\nu\langle v_z^2\rangle)\right\} = 4\pi G\rho_m. \tag{21}$$

Thus, by astronomical observations of $\nu(z)$ and $\langle v^2(z)\rangle$ the value of ρ_0 is determined:

$$\rho_m = \rho_* + \rho_{gas} + \rho_{DM},$$
$$\text{with } \rho_{DM} \approx 0.5\text{–}1\ \text{GeV cm}^{-3}. \tag{22}$$

Notice that Figure 6 is a plot of the square of the rotation velocity versus the radius. Since $V_c'^2 = r\partial\phi/\partial r$, such a parameter is additive and facilitates the separation of various components that contribute to the observed rotation curve.

Distribution of velocities of dark-matter particles

The design and interpretation of any experiment to detect these particles critically depends upon not merely their density but also on the distribution of their

velocities. This distribution is derived by modelling the mass distribution in and around the galaxy in terms of collisionless particles satisfying the Boltzmann equation. The gravitational potential is given by the Poisson equation, with the source term consisting of the sum of the visible matter and that of the dark matter. Unless one has detailed knowledge of the mass distribution up to large distances of several hundred kpc, it is not possible to determine this uniquely.

As a first step start with the stationary collisionless Boltzmann equation

$$\mathbf{v}\cdot\nabla f-\nabla\phi\cdot\frac{\partial f}{\partial \mathbf{v}}=0, \tag{23}$$

and assume that the distribution function for the dark-matter particles takes the form

$$f=\left(\frac{2}{\pi}\right)^{3/2}\frac{n_0}{s^3}\exp[-(\tfrac{1}{2}v^2+\phi)/s^2], \tag{24}$$

which, by virtue of Jeans' theorem, satisfies equation 23. Here ϕ is the total gravitational potential normalized to zero at the centre of the galaxy and n_0 is the number density of the particles of dark matter there. Contributions to the potential ϕ arise from both the density of the visible matter, ρ, which is known in principle, and from the dark matter, which, for reasons of self-consistency, should satisfy

$$\begin{aligned}\nabla^2\phi_{\mathrm{DM}}&=4\pi G\rho_{\mathrm{DM}}=4\pi G\int m f d^3v\\&=4\pi G\rho_0 m\exp[-(\phi_*+\phi_{\mathrm{DM}})/s^2].\end{aligned} \tag{25}$$

Now equation 25 can be solved to determine ϕ_{DM} for any chosen value of s, and since ϕ_{DM} is given we have $\phi(\omega)$. This $\phi(\omega)$ is then used to calculate the rotation curve $V(r)$ of the galaxy using the formula given in equation 18, which is then compared with the observed rotation curve. I carried out a preliminary analysis which has yielded the result

$$s\geqslant 290\ \mathrm{km\,s^{-1}}. \tag{26}$$

This corresponds to $\langle V^2\rangle^{1/2}\approx 500\ \mathrm{km\,s^{-1}}$, somewhat higher than the $300\ \mathrm{km\,s^{-1}}$ adopted conservatively in the analysis of several experimental searches for dark matter. The calculated rotation curve is shown in Figure 6. This model yields a total mass of $5\times10^{12}\ M_\odot$ within 100 kpc of our galaxy, consistent with the estimates given in the review by Faber and Gallagher[5].

The next step is to note that the solar system is moving through this 'gas' of dark-matter particles with a velocity V of about $230\ \mathrm{km\,s^{-1}}$. In this reference frame the velocity distribution takes the form

$$\frac{dn}{dw}=4\left(\frac{2}{\pi}\right)^{\frac{1}{2}}\frac{n_0 w}{sV_0}\{\exp[-(w-v_0)^2/s^2]-\exp[-(w+v_0)^2/s^2]\} \tag{27}$$

or a fluence

$$\frac{dg}{dw}=w\frac{dn}{dw}, \tag{28}$$

which directly determines the count rate in any direct-detection experiment. I shall use this distribution later.

Types of dark matter

There are basically three categories of dark matter, referred to generally as baryonic, hot and cold; besides these there are also several suggestions for possible candidates that we may classify as exotic.

Baryonic dark matter

The problem of baryonic dark matter is closely connected with the successes of studies of primordial nucleosynthesis in explaining the abundances of helium, deuterium and lithium in the universe (see M. S. Turner 1991, ref. 5). As shown in Figure 8 this requires the abundance ratio, η, of baryons to photons in the universe to be constrained in the interval

$$3\times10^{-10}<\eta<5\times10^{-10}, \tag{29}$$

which transforms into the following limits on Ω_b in baryons:

$$\begin{aligned}&0.04<\Omega_b<0.07 \text{ for } H_0=50,\\&0.01<\Omega_b<0.02 \text{ for } H_0=100.\end{aligned} \tag{30}$$

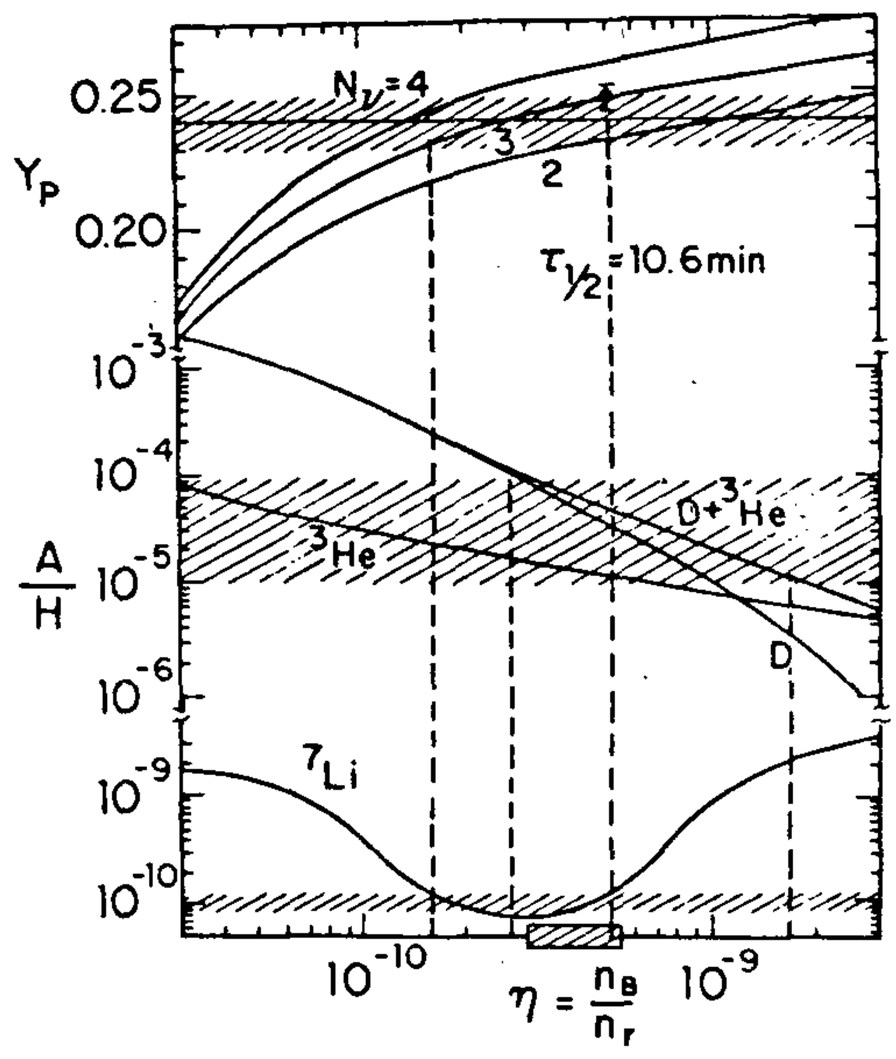

Figure 8. Fraction abundances of elements generated in primordial nucleosynthesis shown against the assumed baryon photon number ratio. The hatched areas are the regions allowed by the observations. (After Turner[5].)

It is interesting to note that these values of Ω_b are larger than $\Omega_{lum} \approx 0.01$ and are closer to the value of $\Omega \approx 0.1$. Thus we are yet to find the baryons that would give rise to the correct ratios of elements synthesized in the big bang. The interesting possibility is that these are present in the form of massive compact objects distributed over the halos of galaxies, including our own. Being primordial, they must predominantly consist of hydrogen and helium and must occur in the mass range

$$10 M_{\odot}^{-7} < M_{b.d.} < 8 \times 10^{-2} M_{\odot}. \quad (31)$$

The lower limit arises when one demands that they should not evaporate away within the age of the universe (see A. De Rujula in ref. 12). The upper limit corresponds to the mass above which these objects would start generating nuclear fusion energy and behave as low-mass stars. Such objects are referred to as brown dwarfs.

Hot dark matter

This type of dark matter was first suggested in the seventies to explain the virial discrepancy of clusters, and is exemplified by light neutrinos[3,4,9,13]. Neutrinos of mass less than 1 MeV stayed in thermodynamic equilibrium with the rest of matter until the universe was about 30 sec old at a temperature of about 1 MeV, and subsequently decoupled and evolved further without any neutrino–antineutrino annihilation. The positrons annihilated and heated up the radiation to increase its temperature by a factor of about 1.4. The fact that neutrinos were in thermodynamic equilibrium allows us to estimate their present-day number density, about 110 cm^{-3} for each flavour, quite accurately.

$$n_{(\nu+\nu)} = 110\ \mathrm{cm}^{-3}. \quad (32)$$

Note that this is much larger than the number density of baryons today:

$$n_b \leq 3 \times 10^{-7}\ \mathrm{cm}^{-3}. \quad (33)$$

Thus, even if these relict neutrinos have a mass of a few eV, they would contribute importantly to Ω. Figure 9 shows how the mass of these particles is bounded by the present-day age of the universe and the value of H_0.

Such particles are called *hot* to signify that at the time of thermodynamic decoupling they were relativistic, and, what is more, the universe was not subsequently heated up substantially through the annihilation of other particles. This means that during the early phases of the universe the mean momenta of these particles were very similar to that of radiation. As the universe expands their momenta scale down with the expansion factor and they become nonrelativistic at an epoch z given by

$$z_{NR} \approx 1000\,(m_\nu/\mathrm{eV}) \approx 20{,}000. \quad (34)$$

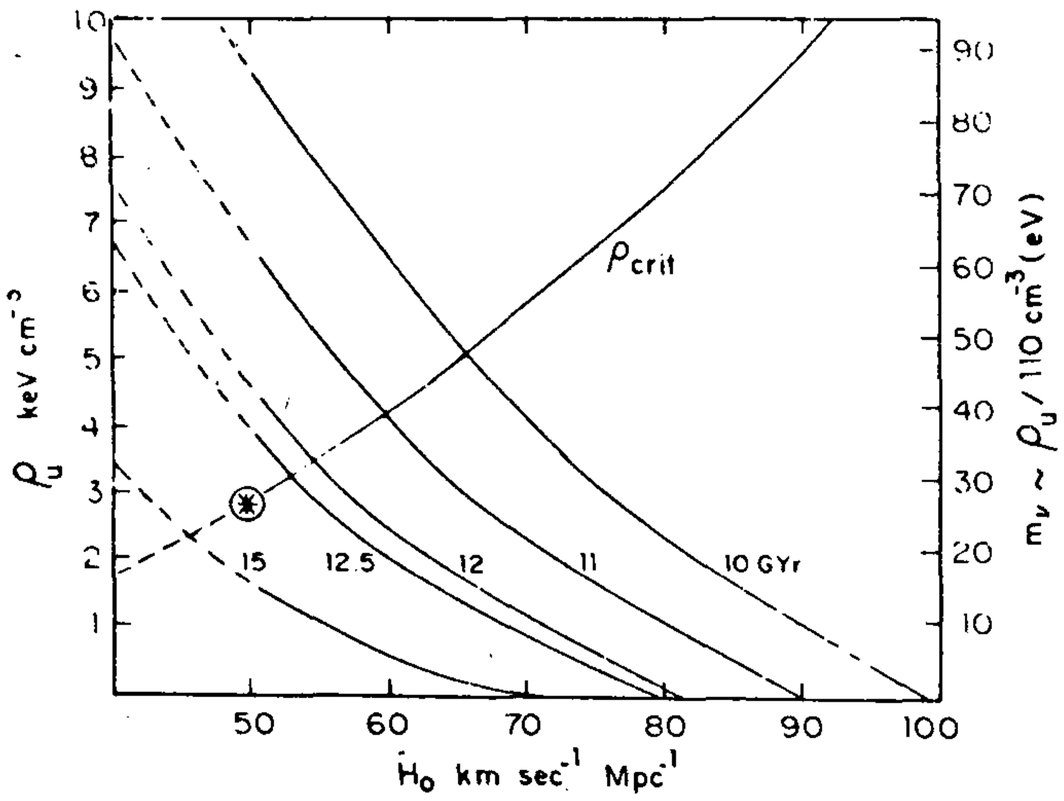

Figure 9. Energy density in the universe as determined by the value of the Hubble constant H_0 and the age of the universe (shown next to the curves in billion-year (Gyr) units). On the right ordinate axis the mass of a neutrino needed to generate this relict density is shown. The asterisk shows the preferred point on this plane.

The primordial perturbations in their density would then start growing into large-scale structures. After the recombination of hydrogen and helium the coupling between matter and radiation in the universe decreases, and matter falls into the gravitational potential wells of dark matter, leading to the formation of galaxies. An important advantage of such a scenario is that since the perturbations in the density of matter start growing only subsequent to its decoupling from radiation, they would not induce unduly high fluctuations and anisotropies in the microwave background. Because of their *hot* nature such particles are most efficient in forming structures on very large scales such as clusters and superclusters.

Cold dark matter

In contrast to the hot relics, the cold relics decouple when they become nonrelativistic. They were first discussed by Lee and Weinberg[14]. Such particles, as long as they are thermodynamically coupled, have abundances that decrease rapidly with temperature with respect to photons as

$$\frac{n_b}{n_\gamma} \sim (m/kt)\exp(-m/kT). \quad (35)$$

Also, the photons increase their number density, heated by the annihilation of various particle states lighter than the relict massive weakly interacting particle under consideration. Subsequent to their decoupling their number density evolves according to the equation

$$\frac{dn}{dt} = -3Hn - \langle \sigma |v| \rangle_{ann} (n^2 - n_{eq}^2), \quad (36)$$

and the present-day number density becomes

$$n(t=t_u) \propto \frac{1}{m\langle\sigma|v|\rangle}. \tag{37}$$

This corresponds to a mass density

$$\rho = nm \propto \frac{1}{\langle\sigma|v|\rangle} \propto \frac{M_w^4}{m^2} \text{ for } m \ll M_w. \tag{38}$$

This ρ is shown in Figure 10. Beyond $m > M_z$ the annihilation cross-section decreases as m^{-2} and the contribution of such particles would increase with m. At very large masses the annihilation cross-section is bound by unitarity to

$$\langle\sigma|v|\rangle_{ann} \leq \frac{8\pi}{m^2}, \tag{39}$$

so that, independent of detailed physics at those masses, such particles, if stable, would contribute excessively to the mass density of the universe. The foregoing argument assumes that for the fermionic components the net fermion number in the universe is zero. Indeed there could be asymmetries generated through CP-violating nonequilibrium processes. If this were so the annihilation cross-sections implied by equations 37 and 38 are lower bounds.

Among the various cold dark-matter candidates that saturate the critical-density bound on the Lee–Weinberg part of the m–Ω plot, a particle of great current interest is the neutralino[15]. This particle is the lowest-mass superposition of four neutral SUSY fermions which mix with one another: $\tilde{B}$ the counterpart of U(1) gauge boson B, $\tilde{W}$ the partner of neutral SU(2) guage boson W, and $\tilde{H}_1^0$ and $\tilde{H}_2^0$ which are the components of the SUSY counterparts of the Higgs. The mass matrix depends on just three parameters: (i) $\beta = \tan^{-1}(V_2/V_1)$, here $V_2 = \langle H_2 \rangle$ gives the mass of the up quark and $V_1 = \langle H_1 \rangle$ gives the mass of the down quark; (ii) the higgsino mass parameter μ; and (iii) the three gaugino masses M_1, M_2, M_3 for U(1), SU(2) and SU(3), where one assumes $M_1 = M_2 = M_3$ at the GUT-scale in the MSSM. Scaling to lower energies with renormalization-group equations yields $M_1 = (5/3) M_2 \tan^2 \theta_w$. One can diagonalize the mass matrix to obtain the neutralino states; the one with the smallest mass can be made stable by ascribing to the SUSY particles an R-parity, which is conserved:

$$\chi_i = z_{i1}\tilde{B} + z_{i2}\tilde{W} + z_{i3}\tilde{H}_1^0 + z_{i4}\tilde{H}_2^0. \tag{40}$$

The other cold dark-matter particle discussed extensively is the cosmion. This particle is expected to have a mass in the interval

$$4\text{ GeV} < m < 10\text{ GeV}, \tag{41}$$

and it is suggested that it is accreted into the Sun in sufficient numbers over the age of the universe. This particle interacts coherently with nuclei, with a typical cross-section of $10^{-36}\,\text{cm}^{-2}$ per nucleon ($10^{-33}\,\text{cm}^{-2}$ on Si). Such a particle would transport energy from the centre of the Sun to the outer regions of the core, thereby lowering the central temperature sufficiently to bring down the ^{8}B-neutrino flux into conformity with Davis' observations.

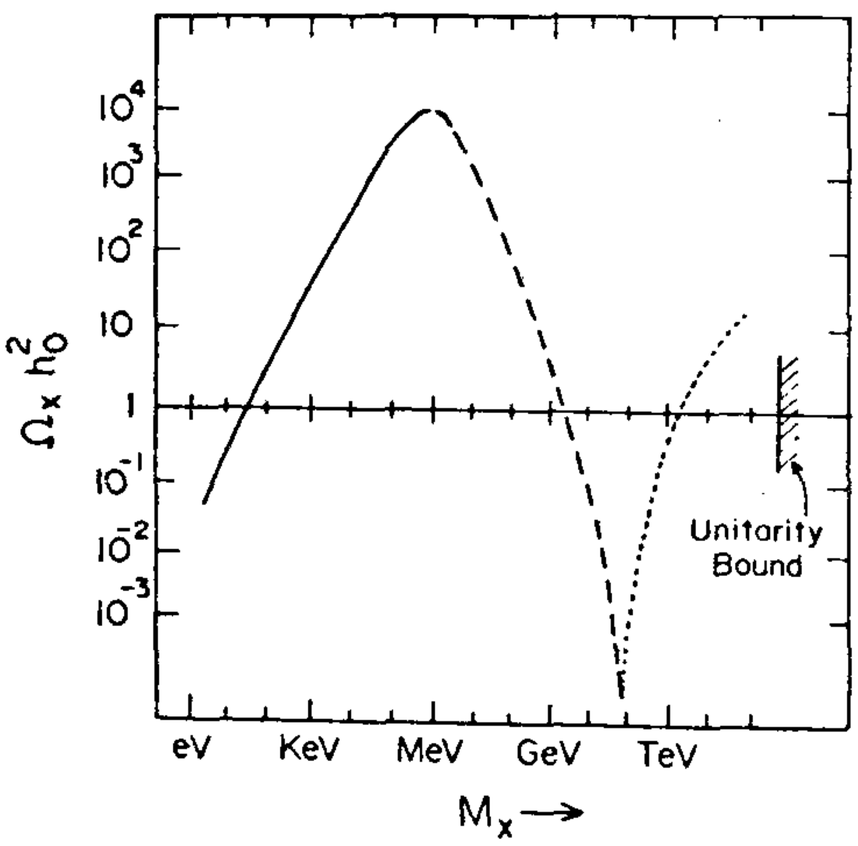

Figure 10. The contribution of weakly interacting particles of various masses to Ω. The dashed line shows the effect of annihilation becoming progressively more important with mass increasing beyond 1 MeV.

Axions

Peccei and Quinn suggested a new symmetry to avoid the so-called strong CP problem in quantum chromodynamics (QCD) which for example leads to an electric dipole moment for the neutron of about 10^{-16} ecm, about 10^9 times larger than the current experimental limits (see review by M. S. Turner[16]). The pseudo Nambu–Goldstone boson associated with the spontaneous breakdown of this symmetry at $f_a \sim 10^{12}$ GeV. The mass of the axion depends on the precise value of f_a and on the PQ charges through a parameter $N(\sim 6)$:

$$m_a = \left(\frac{10^{12}\text{ GeV}}{f_a}\right)\left(\frac{N}{6}\right) \times 3.7 \times 10^{-5}\text{ eV}. \tag{42}$$

The relict density of axions in the universe is generated by three distinct mechanisms:

(i) Thermal production relevant to $m_a > 10^{-4}$ eV occurs soon after the QCD transition, yielding an abundance of about $30\,\text{cm}^{-3}$.
(ii) The first coherent mechanism rests on the fact that the free energy of vacuum depends on the phase angle of the associated pseudoscalar field. Detailed considera-

tions show that this field energy leads to a density

$$\Omega_a h^2 \approx 0.13 \left(\frac{10^{-5}\,\text{eV}}{m} \right)^{1.18}, \tag{43}$$

which would give closure density for $m \sim 10^{-6}$ eV.
(iii) There could be topological defects like strings in the axionic field and these could decay, emitting axions, which could contribute significantly to Ω if m_a is about 10^{-2}–10^{-3} eV. (see Figure 11).

Exotica

Particles like magnetic monopoles with estimated mass of about 10^{16} GeV, cosmic strings, quark nuggets or charged massive particles could in principle contribute importantly. I discuss these briefly at the end.

Experimental searches

Massive compact baryonic objects in our halo

Even though brown dwarfs were considered to be the most likely candidates for the baryonic dark matter, other candidates, like galaxies totally obscured by dust, black holes of mass about $10^2\,M_\odot$, and white dwarfs, are possible. The experimental search for brown dwarfs in our halo (MACHOS, for the whimsical) relies on the gravitational effect these have on the images of stars that lie beyond them in external galaxies such as the Large Magellanic Cloud (LMC). The gravitational microlensing causes the intensity of stellar images to fluctuate. A search for this phenomenon is being carried out by several groups (in Saclay, Lawrence Berkeley Laboratory, Lawrence Livermore Laboratory, Centre for Particle Astrophysics, Steward Observatory). When a star in LMC is perfectly aligned behind a brown dwarf in our halo the microlensing image is a ring whose radius is given[12] by the formula

$$R_E = \left\{ \frac{4GM}{c^2} Dx(1-x) \right\}^{\frac{1}{2}}, \tag{44}$$

where $D \approx 55$ kpc is the distance to the LMC and x is the distance to the brown dwarf in units of D. In the general case where the light ray has an impact parameter d with the brown dwarf the transverse distance varies with time owing to transverse velocities of the star and the brown dwarf. Defining u as this traverse distance in units of R_E we have

$$u_T = \left\{ \frac{d^2 + v_T^2 t^2}{R_E^2} \right\}^{\frac{1}{2}}, \tag{45}$$

and the image magnification consequently varies as

$$A(t) = \frac{u_T^2 + 2}{u\sqrt{u_T^2 + 4}}. \tag{46}$$

By measuring $A(t)$ we can deduce m, v_T and b (see Figure 12). The typical duration of an event is

$$\Delta t \approx \frac{R_E}{V_T} \approx \left(\frac{M}{0.1\,M_\odot} \right)^{\frac{1}{2}} \left(\frac{300\,\text{km s}^{-1}}{v_T} \right). \tag{47}$$

Current searches, monitoring about a million stars in the LMC, should be able to perform a sensitive search for MACHOS in a couple of years time.

Results from SLC and LEP

The measurement of the properties of the weak-vector intermediate boson Z^0 at SLC and with high statistics

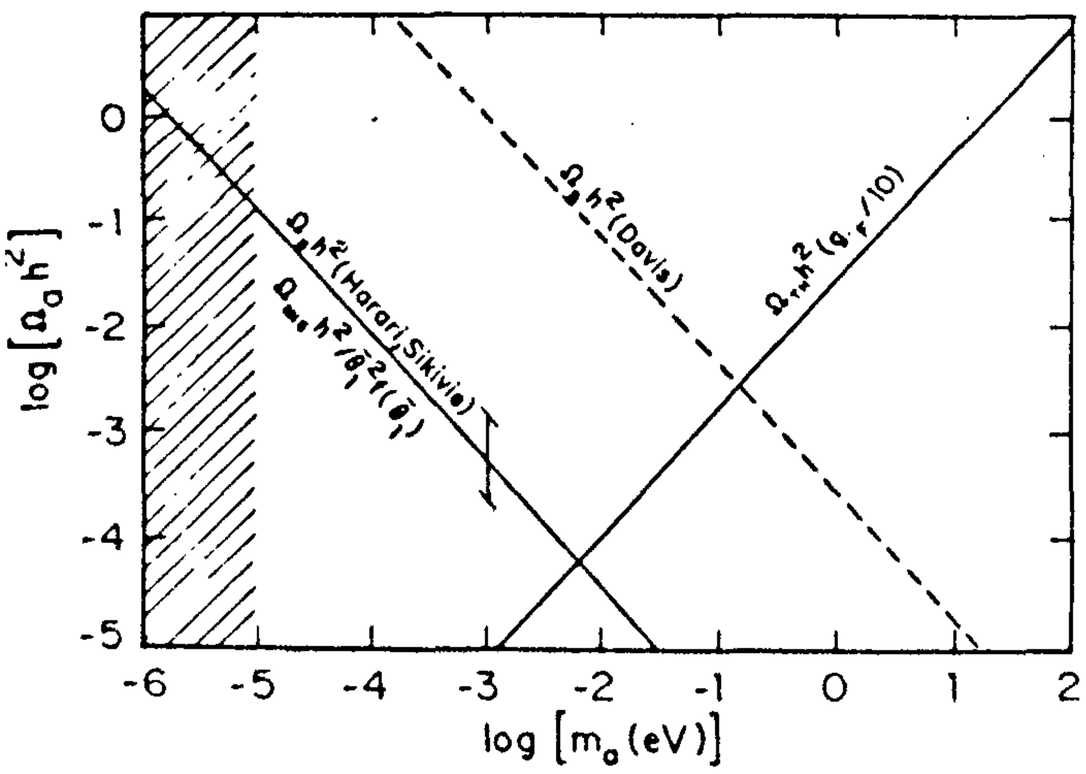

Figure 11. The contribution of axions to the density of the universe (after M. S. Turner[5]). The region where current experimental searches are focused is shaded.

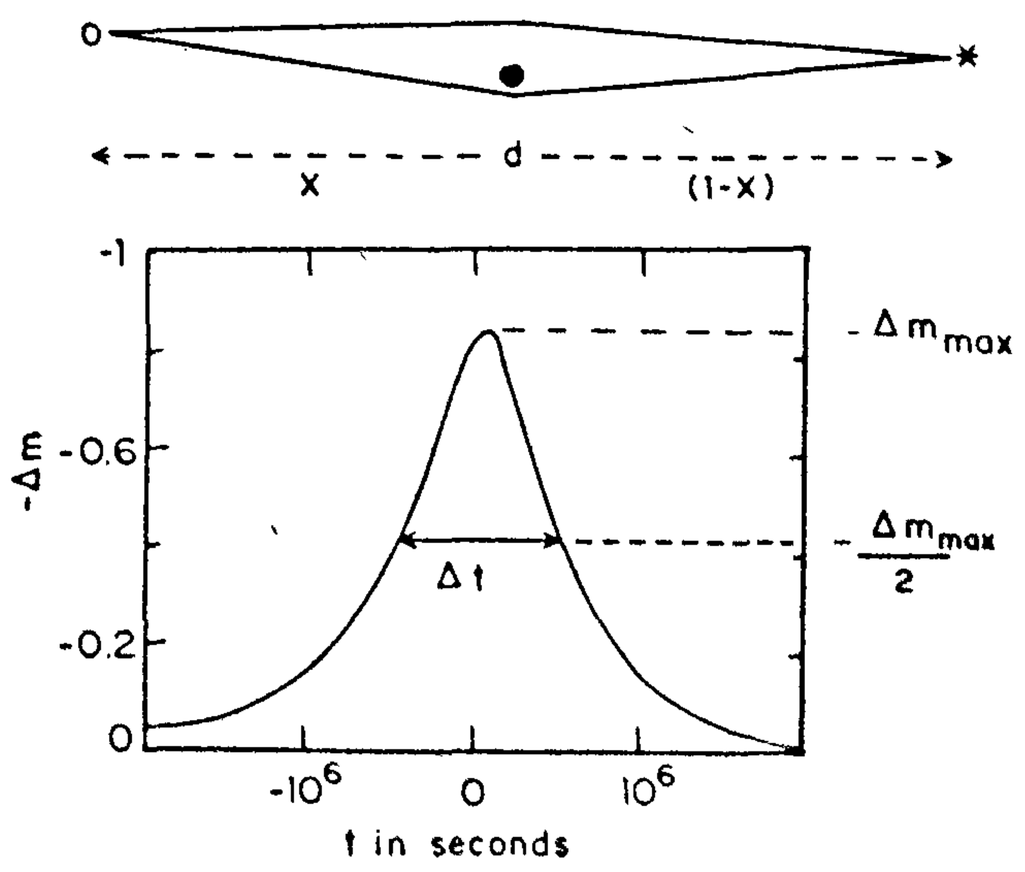

Figure 12. The upper panel indicates how light rays are bent in a microlensing event caused by a brown dwarf. The lower panel shows how the magnitude of a star in the LMC may vary owing to this effect.

at LEP has led to several important results relevant to particulate dark matter[17]. The immense magnitude of the electron–positron storage mugs and the versatility that surrounds the region where e^+ and e^- collide to generate the boson are noteworthy. The most important result of relevance to the topic of dark matter is the line shape shown in Figure 13. Contributions to the width of the resonance arise from hadronic channels, from the charged leptons, and from an invisible component calculable quite accurately for the neutrinos within the standard model; the result is

$$\Gamma_{inv} = \Gamma_z - \Gamma_{had} - 3\Gamma_l = 511 \pm 18 \text{ MeV} \quad (48)$$

$$N_\nu = \frac{\Gamma_{inv}}{\Gamma_l} \cdot \left(\frac{\Gamma_l}{\Gamma_\nu}\right)_{SM} = 3.08 \pm 0.1. \quad (49)$$

This result shows that there are no other light neutrinos besides the three with flavours e, μ, and τ. For massive neutrinos the phase space available in the Z_0 decreases when $2\,m_\nu$ approaches $M_{z^0} = 91.18$ GeV, and the observations exclude any new massive neutrinos with masses below about 45 GeV and also a wide variety of hypothetical particles with weak interactions—such as charginos, L_0, $l^{*\pm}$, ν^*, $\tilde{\nu}$, $\tilde{u}$, $\tilde{d}$, $\tilde{l}$, etc. More to the point are the limits placed on the parameters of the neutralino, χ_0, which is the lowest-mass supersymmetric particle, defined as a linear combination of the two higgsinos, the zino and the bino[17]. Figure 14 shows the bounds obtained on these parameters from the experiments at LEP (see Dydak[18]).

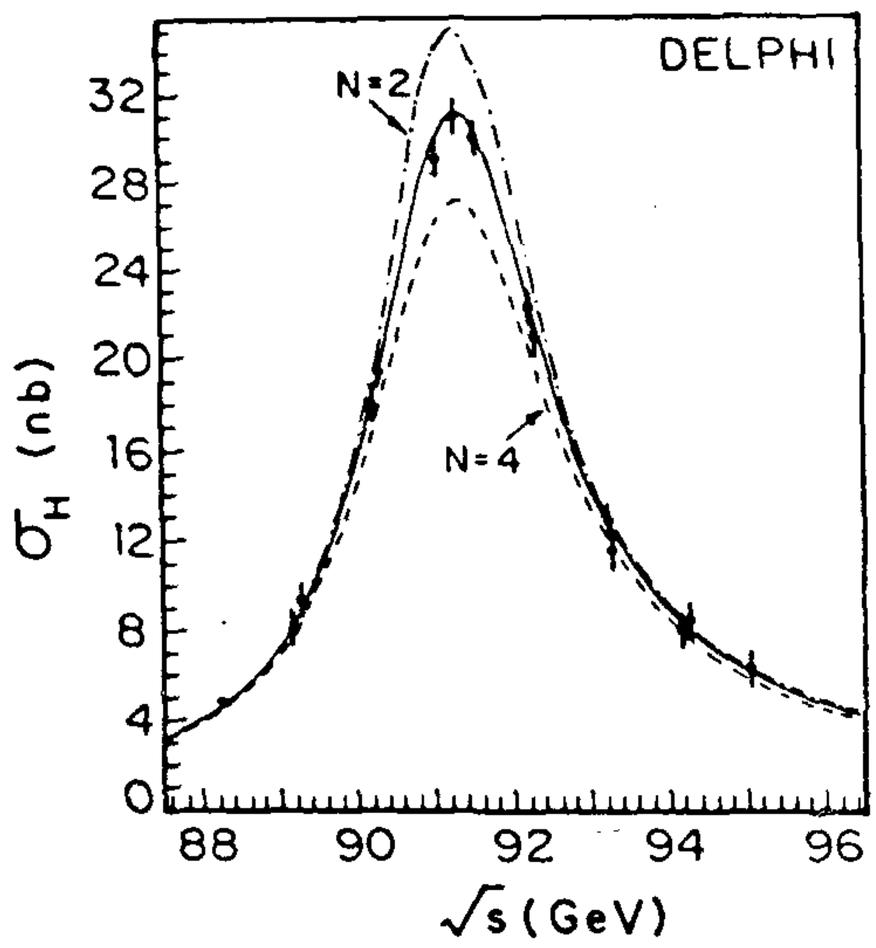

Figure 13. The line shape around the Z^0 resonance measured at LEP by the DELPHI collaboration. The solid line is the best-fit line assuming a contribution of 3.08 neutrinos to the invisible width.

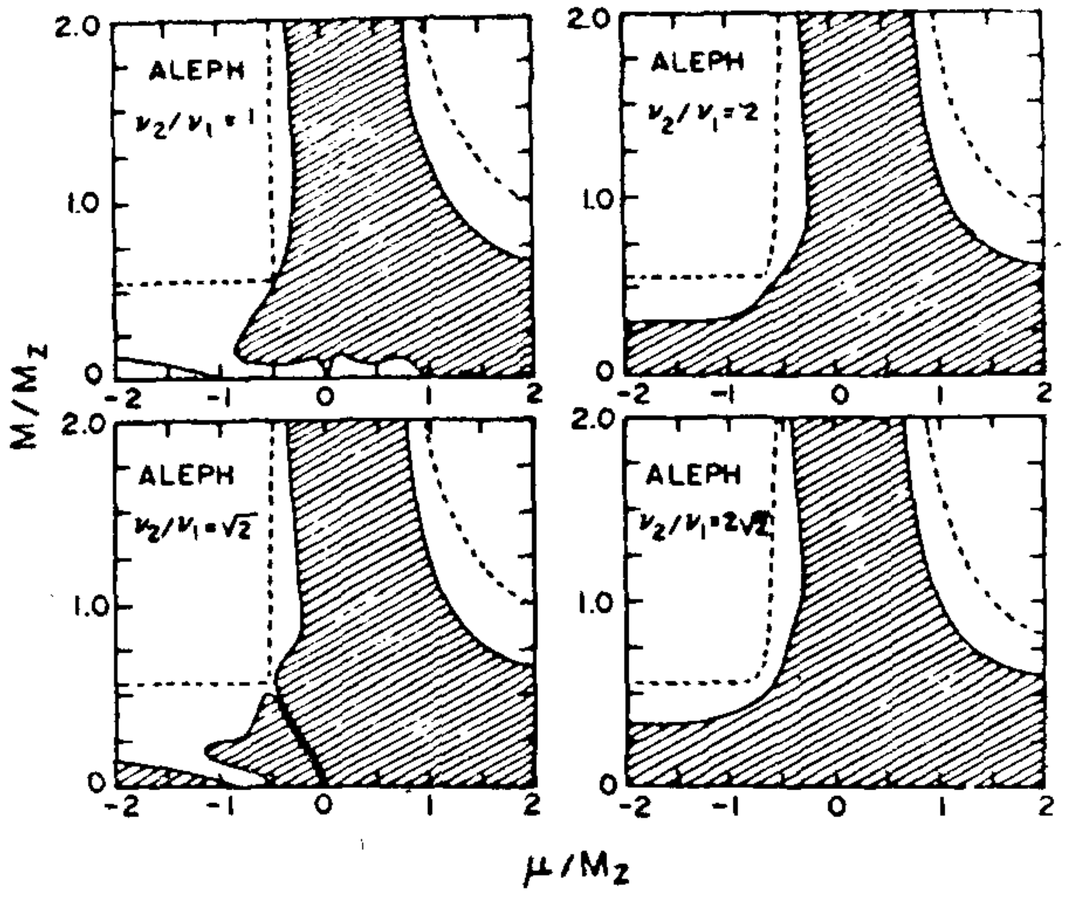

Figure 14. Bounds on neutralino parameters based on ALEPH data.

Three types of searches

As mentioned before the searches for dark-matter particles can be carried out by detection of cosmic radiations generated by them and by 'direct' and 'indirect' methods. The preceding discussion on the Z^0 line shape is an example of the indirect method. I now sequentially take up the various candidate particles and review in each case the import of the various studies carried out by these three methods.

Light neutrinos

These were the first nonbaryonic relicts to be suggested as candidates of dark matter. This suggestion triggered the exciting era of interplay between particle physics, astrophysics and cosmology. While neutrinos are massless in the standard model the cosmological bound on their masses is

$$\sum_i m_{\nu_i} < 30 \text{ eV}. \quad (50)$$

(i) Table 2 shows attempts at determination of the ν_e mass by looking at the high-energy end on a Kurie plot of the β-spectrum[19]. The quoted upper bound is

$$m_{\nu_e} < 9.4 \text{ eV}. \quad (51)$$

Table 2. Recent results from tritium β-decay experiments.

Experiment	Best-fit m_ν^2	Upper limit on m_ν
Los Alamos	$-147 \pm 55 \pm 58$	9.4 eV
Zurich	$-158 \pm 150 \pm 103$	15.4 eV
Tokyo	$-82 + 87 \pm (\ )$	$11 + (\ )$ eV

The first error is statistical and the second error is systematic. Systematic errors are being studied.

However, note that in all the three experiments the best-fit value of $m_\nu^2 \approx -158 \rightarrow -82\,\text{eV}^2$. To be most conservative we should use this as the zero of the scale, in which case the limit relaxes to

$$m_{\nu_e} < 15\,\text{eV}. \tag{52}$$

(ii) Double β-decay could take place without the emission of any neutrinos should they be Majorana particles with mass. The sum of the energies of the β-particles is equal to the Q value of the decay and consequently provides a clear signature for the process. The results from the UCSB-LBL experiment[20] on the system $^{76}\text{Ge} \rightarrow {}^{76}\text{Se} + 2\beta + 2\nu/0\nu$ are shown in Figure 15. The bound on the Majorana mass of the neutrino, taking into account the newly measured Q value for the decay and the uncertainties in the decay matrix elements, is given by

$$[m_{\nu\text{-Majorana}}] \equiv \{\Sigma \text{sign}_i\, u_{ei}\, m_i^2\}^{\frac{1}{2}} < 4.7^{+0.8}_{-0.5}\,\text{eV}. \tag{53}$$

It is important to note here that the mass limit that appears in the above equation is actually an effective mass estimated from the mass matrix of all the three neutrinos.

(iii) Solar neutrinos provide a clue to the neutrino masses if the MSW mechanism is indeed the cause of the low count rates in the Cl and Ga experiments[21]. An analysis which includes the results of a real-time detection of the solar neutrinos at Kamiokande, the Cl and Ga experiments is shown in Figure 16 which suggests ($|\Delta m^2| \approx 10^{-6}$; $\sin^2\theta \approx 10^{-2}$) for $\nu_e\,\nu_\mu$ mixing[22]. This leaves us the possibility that only ν_τ is really massive if the cosmological bound is to be saturated by a light neutrino. There is a possibility that the ν_τ and ν_ν may mix with a larger Δm^2 but with $\sin^2\theta_m \leq 10^{-4}$, experiments are under way with high energy ν_μ beams to test this possibility.

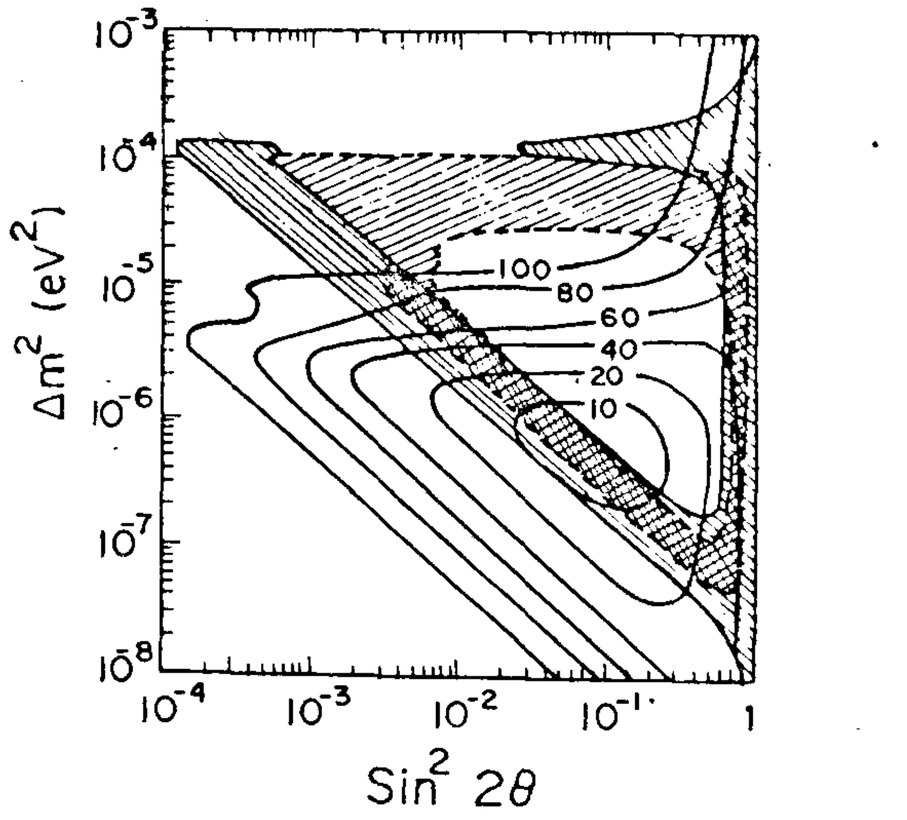

Figure 16. Regions in the $\sin^2\theta$, δm^2 plane allowed by the observations of solar neutrinos by the Cl experiment, by direct scattering experiments at Kamioka, and by the Ga experiment performed by the SAGE collaboration. The three results when taken together suggest a region around $\sin^2\theta \sim 3 \times 10^{-2}$ and $\Delta m^2 \sim 10^{-6}\,\text{eV}^2$.

(iv) Sciama[23] has recently argued that the mass of ν_τ could be in the range of about 25–30 eV and its radiative decay with a lifetime of $\sim 10^{23}$ s would generate enough UV photons of energy $m_\nu/2$ to account for the ionization of hydrogen in the galaxy. This decay rate narrowly escapes the earlier bounds on it placed by Cowsik, Henry, Turner and others (see ref. 24). However, the recent data obtained by Davidson *et al.*[25] using the Johns Hopkins UV telescope aboard the space shuttle rule-out this attractive suggestion, as shown in Figure 17.

(v) Direct observation of cosmic neutrinos has been

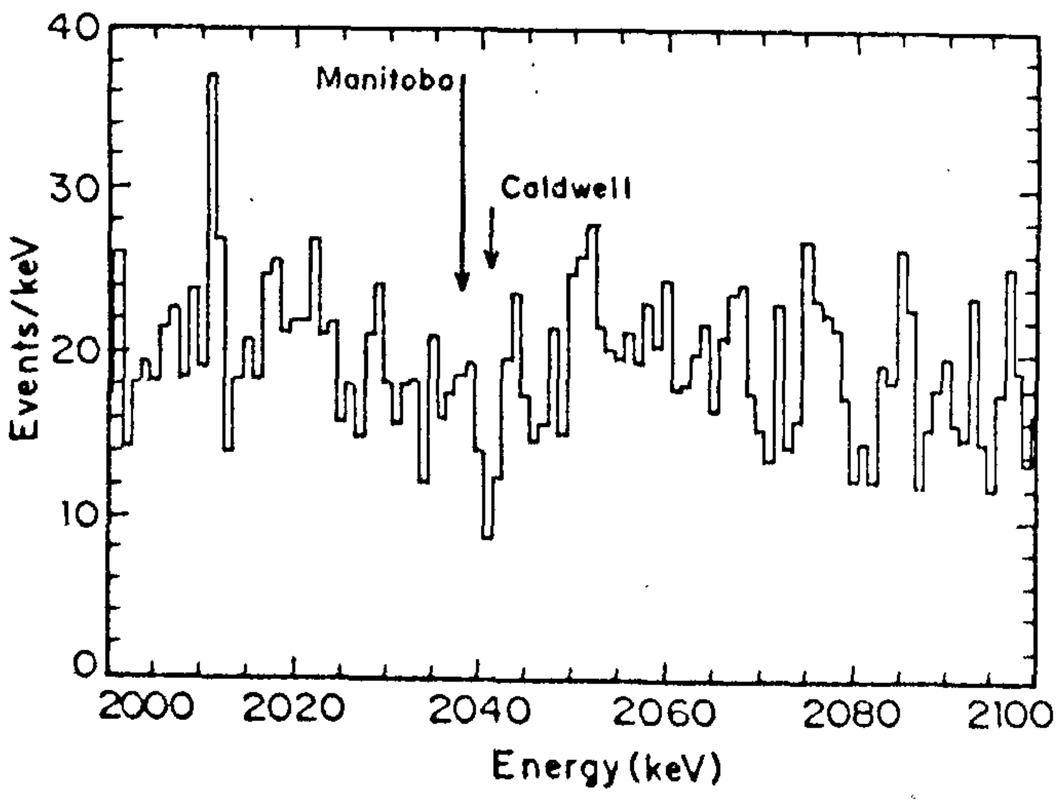

Figure 15. Spectrum of events recorded in a germanium crystal in a band encompassing the expected position of the peak should neutrinoless double β-decay occur. The recent redetermination of the Q value by the Manitoba group relaxes the bounds on the Majorana mass of the neutrino set earlier by Caldwell *et al.*[20]

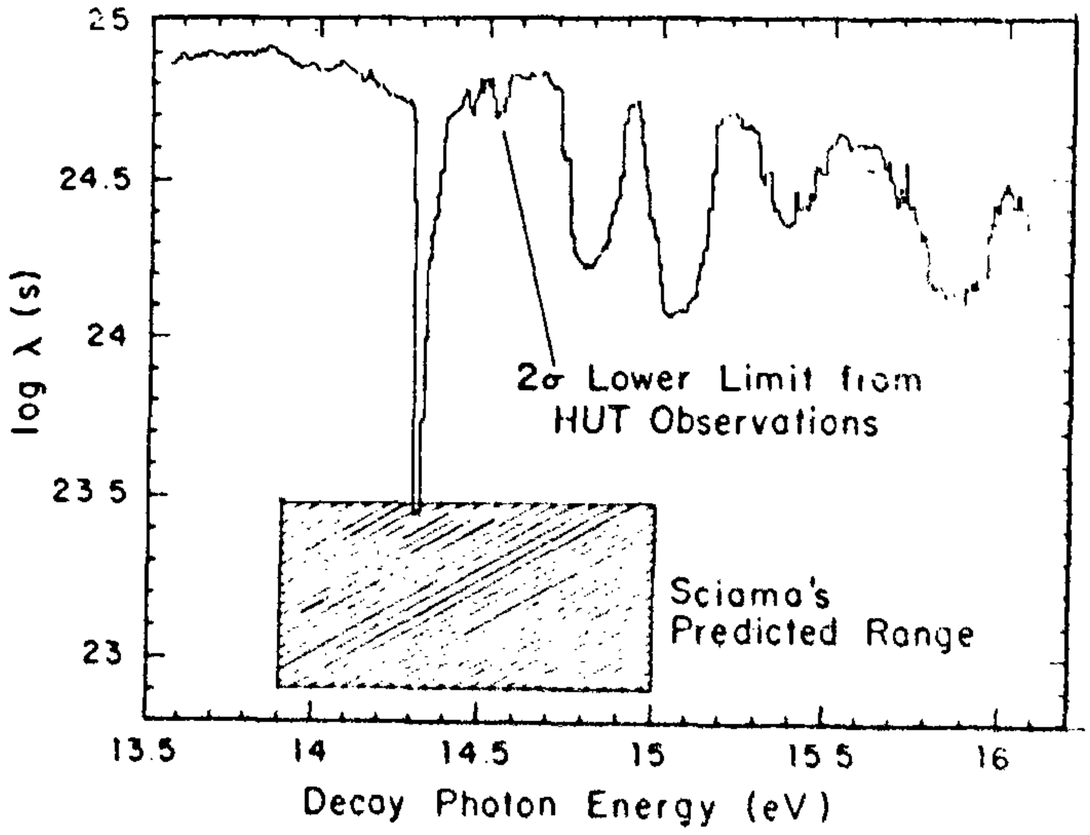

Figure 17. The 2σ lower bounds derived from the observations of UV line intensities from the rich cluster of galaxies ABEL-665 exclude the range of neutrino mass and lifetime suggested by Sciama to explain the ionization of galactic hydrogen. (Figure reproduced from Davidson, A. F. *et al.*, *Nature*, 1991, **351**, 128.)

discussed by Cowsik[26] and by Smith and Lewin[27]. They consider the possibility of coherence in their scattering over macroscopic dimensions of about 20 μm corresponding to their de Broglie wavelength. The sensitivities of the detectors built to date are inadequate by a factor of about 10^9 for seeing any such signal in the near future.

(vi) It would be interesting to discuss the wide variety of suggestions triggered by the recent experiments that suggest the possible existence of a 17-keV neutrino mixing with the standard ν_e at 0.5% level. I do not discuss these here.

WIMPs

There are cold dark-matter particles that saturate the mass bounds given in Figure 10 in the Lee–Weinberg part of the diagram.

(i) The LEP–SLC experiments on Z^0 width clearly rule out Dirac neutrinos lighter than 43 GeV.

(ii) The double β-decay experiments rule out massive neutrinos up to TeV unless they occur in pairs with opposite CP and suitable mixing parameters so as to contribute negligibly to $\langle m_\nu^2 \rangle$.

(iii) I now focus on the neutralino, which is stable, being the lightest of the SUSY particles. Those combinations of neutralinos which couple to Z^0 are ruled out up to masses of 43 GeV. We saw earlier the regions of the parameter space excluded by the LEP data. The experiments at the $\bar{p}p$ collider (CDF) at Fermilab set a lower limit on the gluino mass,

$$M_3 > 120 \text{ GeV}, \tag{54}$$

which translates, along with the LEP results, to a limit

$$m_\chi > 20 \text{ GeV} \tag{55}$$

when one assumes $M_1 = M_2 = M_3$ at the GUT scale (refs. 15, 18). Relaxing these constraints would make more of the parameter space available. Also, if the χ_0 does not couple to Z^0 then the possibility that it would scatter off nuclei coherently would become unlikely—thus making the direct-detection experiments very difficult[28].

The direct searches for weakly interacting massive particles (WIMPs) have been performed with semiconductor ionization detectors, which should be of high purity to reduce the radioactive background. Also, extreme care is needed to shield the detector from cosmic rays, radioactivity, etc. As noted earlier there would be a fluence of particles which constitute the galactic dark matter (see equation 27). These particles would scatter off the nuclei in the detector, coherently if the dark-matter particles have a vector coupling, with a cross-section which increases quadratically within the nuclear mass as

$$\sigma \approx \frac{\sigma_0}{m^2} \frac{m_x^2 m_N^2}{(m_x + m_N)^2}. \tag{56}$$

In the scattering process the WIMP transfers part of its energy to the nucleus, which on the average is given by

$$\varepsilon \approx \frac{m_x m_N}{(m_x + m_N)^2} m_x w^2. \tag{57}$$

A small fraction of this energy, $\delta \approx 0$, 2–0.4, appears as ionization energy, which can be amplified and recorded. The major fraction of ε goes into phonons which eventually get thermalized and leads to an increase in the temperature of the detector. Writing the ionization energy as η,

$$\eta = \delta \frac{m_x m_N}{(m_x + m_N)^2} m_x w^2 = \mu w^2. \tag{58}$$

The expected pulse-height distribution is given by

$$\frac{dn}{d\eta} = 2\left(\frac{2}{\pi}\right)^{\frac{1}{2}} \frac{\rho_0 \sigma}{m_x s V_0} \left(\frac{\eta}{\mu^3}\right)^{\frac{1}{2}} \times \left\{ \exp -\tfrac{1}{2}\left[\frac{(\frac{\eta}{\mu})^{\frac{1}{2}} - V_0}{s}\right]^2 - \exp -\tfrac{1}{2}\left[\frac{(\frac{\eta}{\mu})^{\frac{1}{2}} + V_0}{s}\right]^2 \right\}. \tag{59}$$

We note that as the spread in the particle velocities, s, increases the integral count rate increases for the same density ρ_0, because of the increase in the mean velocity and thus the fluence. The distribution also broadens and the pulse-height distribution shifts to higher energies, making it more easily accessible to measurement (see Figure 18). For $m_x < m_N$, increasing m_x merely broadens the distribufion and lowers its amplitude as the flux decreases for the same ρ_0. This event rate in

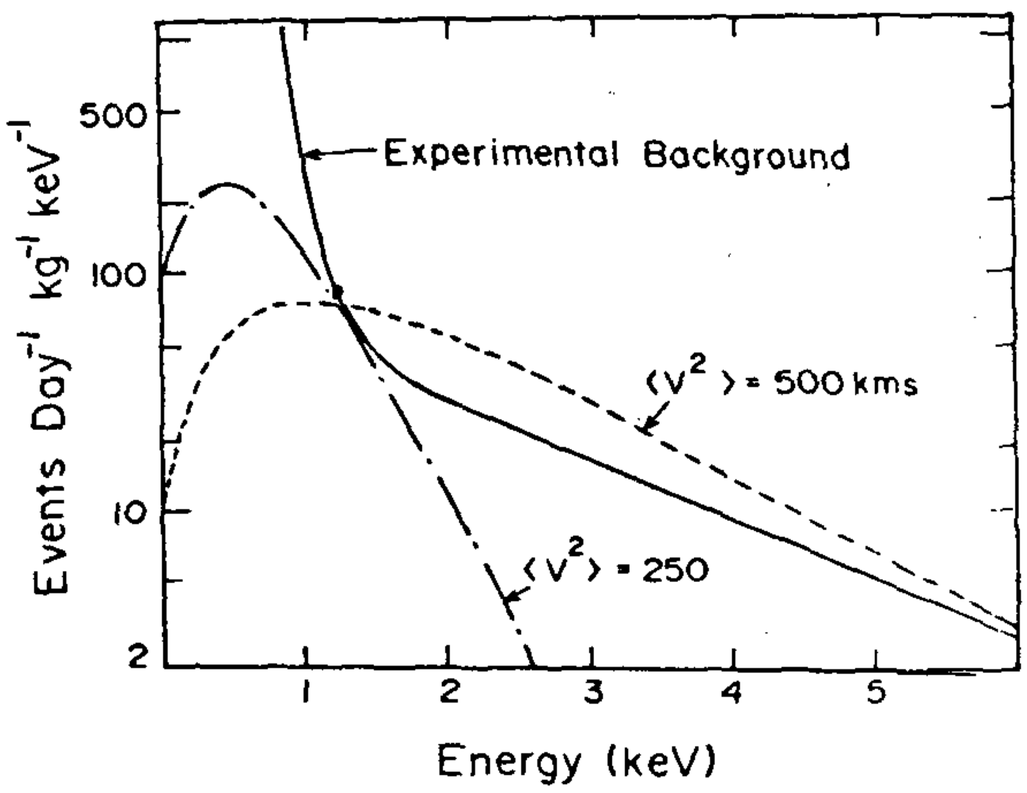

Figure 18. The dependence of the expected spectrum of events due to scattering of cold dark-matter particles in a germanium detector on the assumed dispersion in their velocities compared with the background produced by radioactivity and other sources.

equation 59 is to be added to the background count rate expected in the detector and should be compared with the actual count rate; Figure 19 shows such a comparison. The experiments essentially rule out all particle candidates with weak interactions in the mass range 10 GeV to 4000 GeV for $\langle V^2\rangle^{1/2} \approx 300\ \mathrm{km\ s^{-1}}$ and the lower limit shifts to ~ 2 GeV for $\langle V^2\rangle^{1/2} \approx 500\ \mathrm{km\ s^{-1}}$. Notice in particular that the cosmions, which were proposed to transport energy in the core of the Sun and thereby solve the solar neutrino problem as well as the dark matter problem, are also ruled out. Figure 20 is an overview of the bounds obtained by various direct scattering experiments.

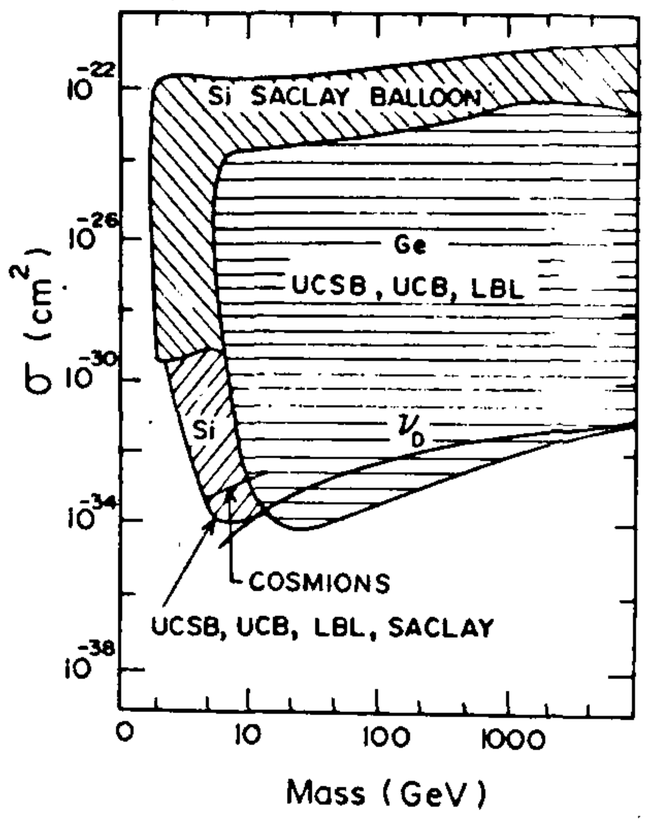

Figure 20. An overview of the bounds obtained by direct experiments on the scattering cross-section of the particles of dark matter populating the galactic halo.

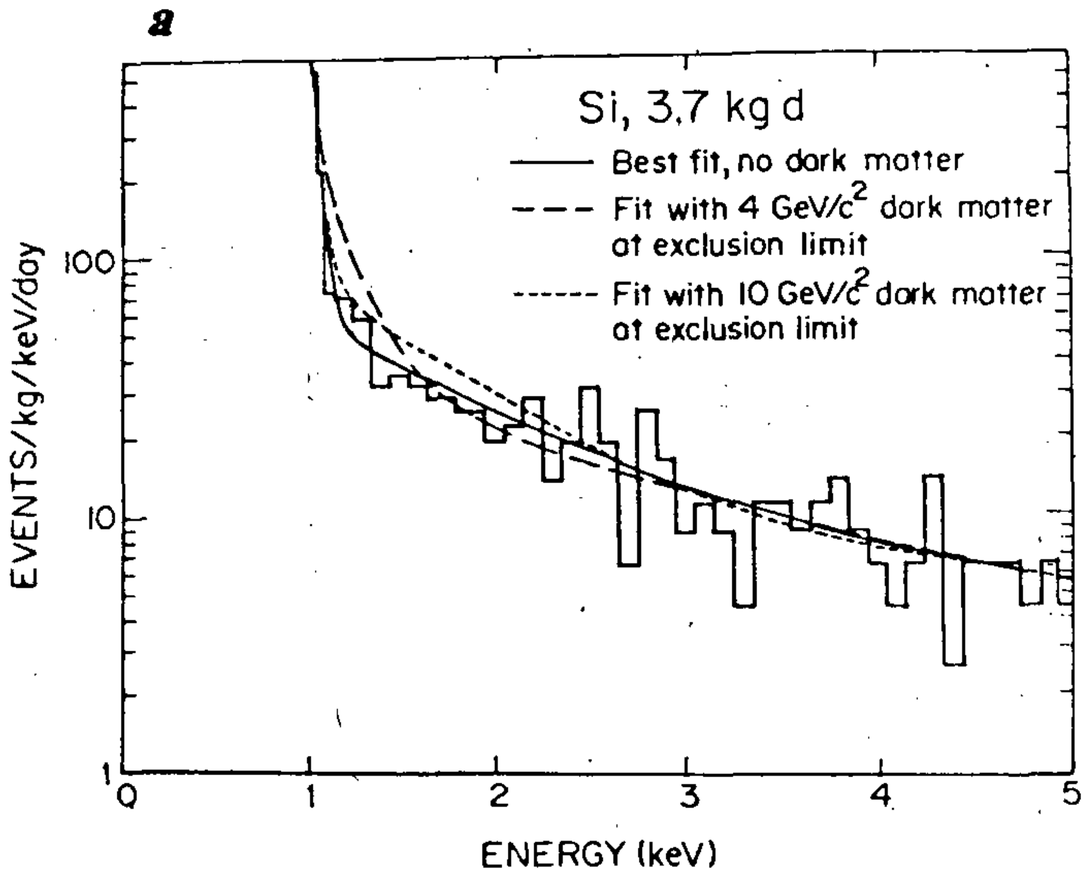

Figure 19. ***a***, Comparison of the experimentally measured background in a Si–Li detector with the theoretically expected spectrum[5]. ***b***, Upper bound on the scattering cross-section of the cold dark-matter particles constituting the galactic halo. If the dispersion in their velocities is larger than the labelled values the limits improve as indicated by the arrows.

WIMP annihilation and the galactic halo

The annihilation of WIMPs in the halo of our galaxy would give rise to a source of γ-rays, $e^{\pm}$ and $\bar{p}p$ generated through the processes

$$\begin{aligned} &\chi\bar{\chi} \to q\bar{q} \to \pi^0, \eta, \ldots, \to \gamma \ldots \text{ (continuum)} + \\ &\chi\bar{\chi} \to \gamma\gamma \text{ (line)} \\ &\chi\bar{\chi} \to q\bar{q} \to p\bar{p} + \cdots \\ &\chi\bar{\chi} \to e^+e^-. \end{aligned} \tag{60}$$

Clearly the exact calculation of the rates of the above processes requires precise knowledge of the physics of the particles comprising dark matter. One aspect of the problem leads to some simplification: in order that these particles contribute effectively to the present matter density of the universe, i.e. $\Omega_\chi \approx 1$, their annihilation rate $\langle\sigma|v|\rangle$ is fixed by the equation 38.

Gamma-ray background

Following the efforts of Rudaz and Steaker, Ellis *et al.*, Freese and Silk, and Stecker and Tylkar[29] (see also the review by Freese[5]), the continuum photon flux in the direction (l, b) in the galaxy will be

$$\phi(E_\gamma) = \frac{1}{4\pi} n_\chi^2 \langle\sigma_a|v|\rangle h \phi(E_\gamma) J(l,b). \tag{61}$$

Here $\phi(E_\gamma)$ is the spectrum expected from a single annihilation, a the core radius of the WIMP distribution in the galaxy, and $J(l,b)$ the normalized integral along (l,b) of the square of the WIMP density normalized to its central value h.

In Figure 21 this flux is shown for a typical direction

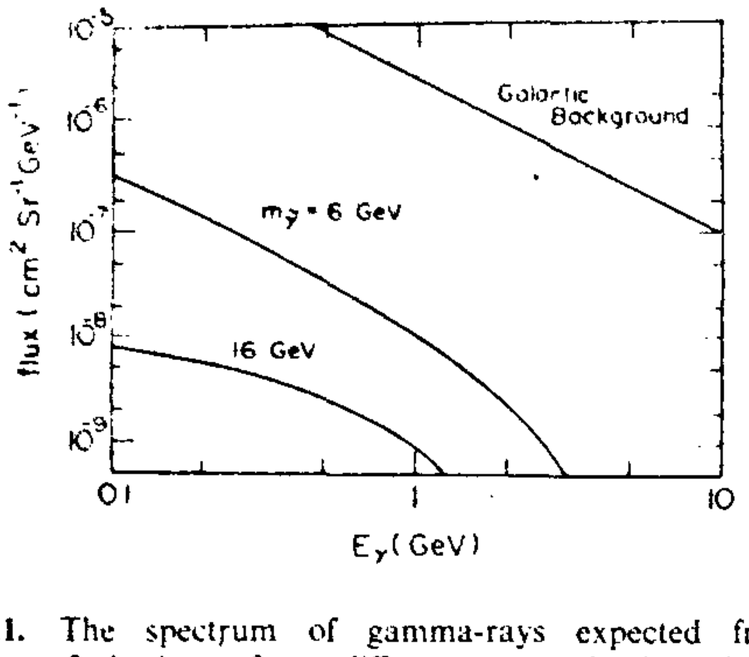

Figure 21. The spectrum of gamma-rays expected from the annihilation of photinos of two different masses in the galactic halo compared with the galactic background. (After Stecker and Tylkar[29].)

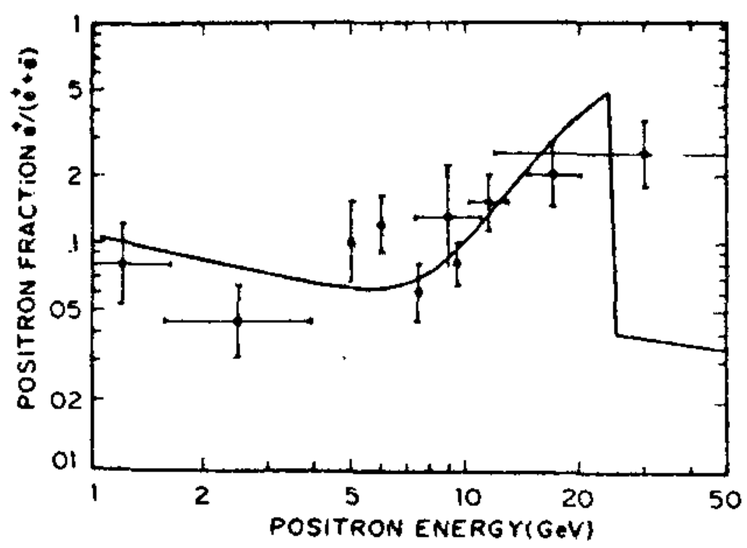

Figure 22. Theoretical prediction of the shape of the positron fraction in cosmic rays generated by the annihilation of cold dark-matter particles in the galactic mass superimposed on the observed spectrum; the normalization is arbitrary and the contribution from dark-matter annihilation is expected to be very small. (After ref. 30.)

($l \approx 45$; $b \approx 45$) and is compared with the background flux generated by the galactic disc. The shape of $J(l, b)$ allows this diffuse component to be characterized and should be within the capabilities of the Gamma Ray Observatory (GRO).

A clearer signal is expected if the final state in $\chi\bar{\chi}$ annihilation is a two-body one as this would give rise to a *monochromatic* γ-ray line. I should point out that the line would have a low-energy wing ($\phi(\dot{E}_\gamma) \sim E_\gamma^2$ for $E_\gamma < E_{max}$) arising from redshifted contributions from external galaxies. The intensity of such a line would be too small to be seen by the GRO but future missions may be able to pick up such a signal.

Positrons and cosmic rays

Since $\chi\bar{\chi}$ can annihilate directly into e^+e^- pairs it would give rise to a sharp enhancement in the cosmic-ray positron flux at the χ mass. The expected flux behaves like

$$f \sim \frac{c}{4\pi}\left(\frac{\rho_0}{m_\chi}\right)^2 \langle \sigma_a |v| \rangle \tau_{CR}. \qquad (62)$$

Of course the synchrotron and the Compton energy losses will spread the sharp peak in the production spectrum to lower energies. Even though the expected fluxes are quite small[30] it is interesting to compare the expected shape of the $e^+/(e^+ + e^-)$ ratio with that observed in cosmic rays, as shown in Figure 22.

Antiproton flux

The primary annihilation process is into $q\bar{q}$ pairs which evolve out of the interaction region as jets containing a fraction of about 10% of nucleon-antinucleon pairs. For $m_x \geq 20$ GeV the theoretically expected continuum fluxes are again quite small, a factor of 10^3 down with respect to the upper bounds set by cosmic-ray observations, as shown in Figure 23.

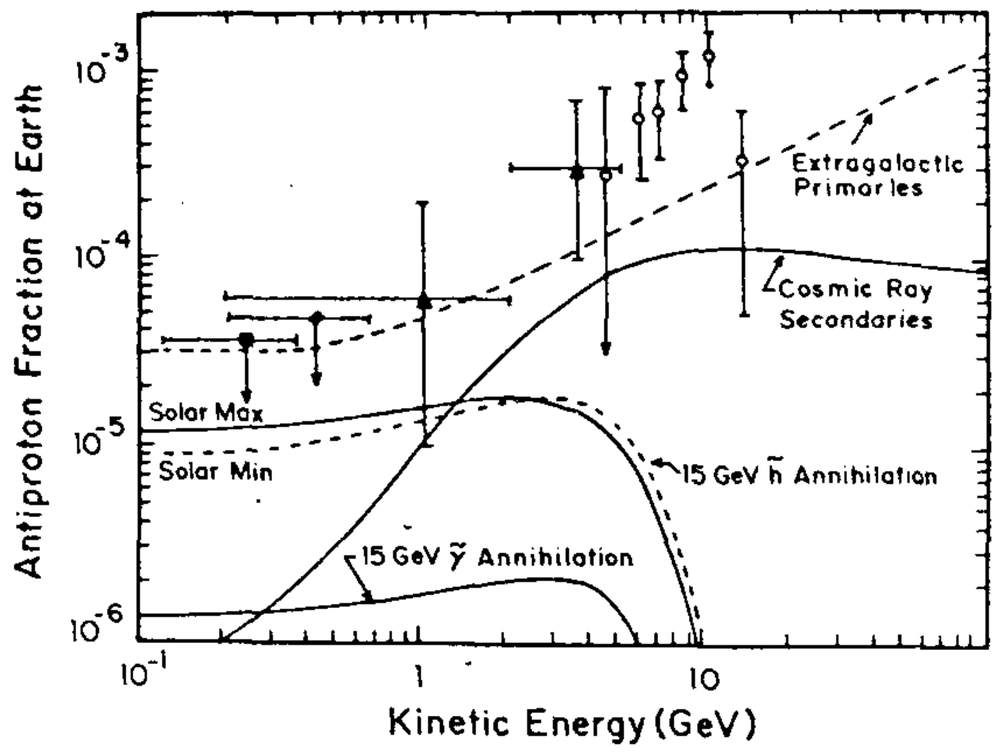

Figure 23. Contribution of photino and higgsino annihilations in the halo to the antiproton flux in galactic cosmic rays. The masses of these particles are expected to be much larger than the 15 GeV value assumed in the calculations. (After the review by Freese, see ref. 5.)

Annihilation of WIMPS in the Earth and the Sun

The WIMPs would be accreted by planetary and stellar bodies like the Earth and the Sun. These would scatter further and would sink to the core, and thus concentrated would annihilate effectively (see Figure 24). None of the annihilation products other than the neutrinos could escape from these regions, of course. The capture rate and annihilation rate would balance, giving rise to a potentially observable flux of neutrinos from both these sources. The capture rate is given by

$$C = \frac{A\rho_{0.3}}{v_{300}} \sum \frac{f_i x_i (\sigma_i / 10^{-36}\ \mathrm{cm}^2)}{m_x m_i / \mathrm{GeV}^2}, \qquad (63)$$

where f_i is the mass fraction of element i with mass m_i and x_i is an efficiency factor. The constant $A_\odot \approx$

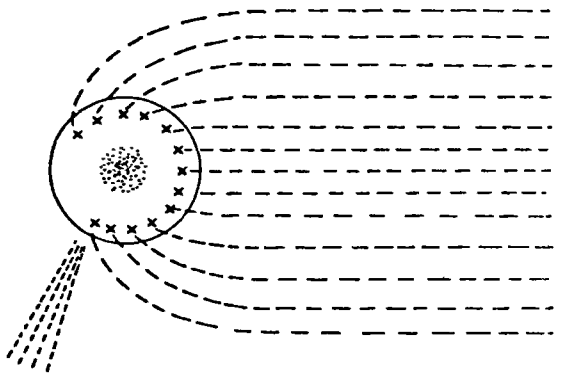

Figure 24. Accretion of cold dark-matter particles by the Earth and the Sun shown schematically. Their subsequent annihilation generates a flux of high-energy neutrinos of sufficient intensity to be observable by present-day detectors for reasonable assumed masses for the cold dark-matter particles.

$6\times10^{28}\,s^{-1}$ and $A_{\oplus}\approx 6\times10^{19}\,s^{-1}$. Once the annihilation rate, which is identical to the capture rate given in equation 63, is known, the neutrino flux calculation depends on the details of the particle physics, branching ratios, etc. Figure 25 shows the bounds placed by such studies by Kamionkowsky[31].

To summarize: For SUSY particles like the neutralino the experimental limits are quite stringent as long as one stays within the minimal supersymmetric standard model. Outside that the parameters can be so tuned as to escape detection by the various methods described thus far even for relatively small values of the χ-mass.

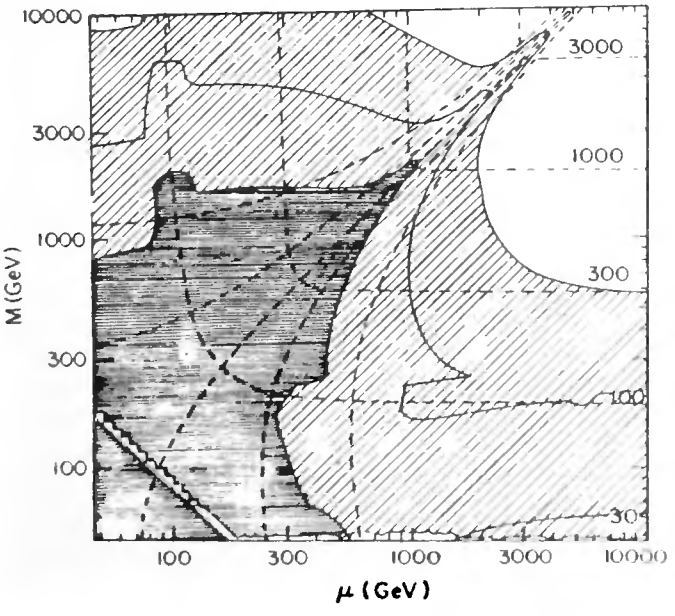

Figure 25. The heavily shaded region of the parameter space of neutralinos is ruled out by the experimental bounds on the high-energy neutrino flux from the Sun. The highly shaded region represents the extended region of sensitivity accessible with future detectors of neutrino astronomy. (After Kamionkowski[30].)

Axions

A variety of particle physics, neutrino physics and stellar physics considerations (including the observations from supernova SN 1987A) rule out axions of mass greater than 10^{-3} eV (ref. 15). As noted earlier this region is interesting from the point of view of dark matter as the coherent mechanisms and string decay can contribute $\Omega_a\approx1$ at the $m_a\sim10^{-6}$ eV and $m_a\sim10^{-3}$ eV respectively. Experimental detection of axions with a mass $\sim10^{-6}$ follows the suggestion by Sikivie (see ref. 16), among others, that its coupling to the electromagnetic fields in a cavity would lead to increase in the number of microwave photons inside. Recent experiments[32] make use of detectors consisting of a high-Q microwave cavity immersed in liquid helium and fermented by a strong magnetic field. The cavity was tuned to various frequencies by dielectrics inside and the noise power within successive cavity bandwidths was spectrum-analysed and the spectrum searched for narrow peaks resulting from axion-to-photon conversion within the cavity. The upper bounds obtained by these experiments in the band 4×10^{-6} eV $<m_a<2\times10^{-5}$ eV are shown in Figure 26. These fall short in sensitivity by a factor of about 1000 in detecting the halo density of axions. Improved searches are under way — what is needed is an equivalent of 1000 detectors rather than a single one 1000 times the volume! This is to keep resonance frequency of the cavity unchanged so that it is sensitive to the same range of axion masses.

Exotica

Now I consider a few dark-matter candidates that are within the realm of possibility but are not specifically motivating on theoretical or observational grounds as specific candidates of dark matter.

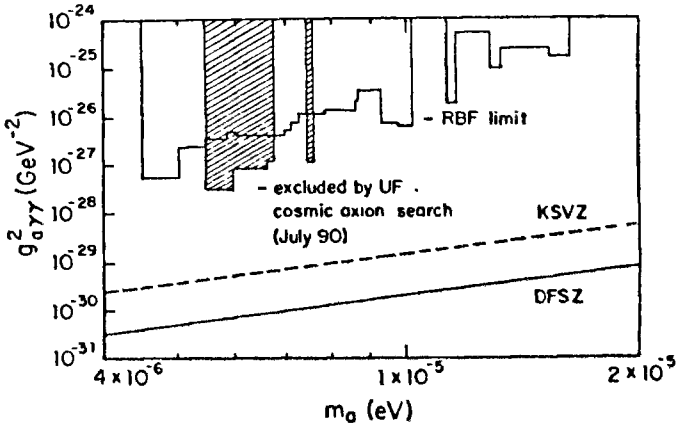

Figure 26. Experimental upper bounds on the axion photon coupling, along with the theoretical expectations. The experiments are as yet insensitive by a factor of about 1000 in detecting a hypothetical background of galactic dark matter consisting of axions.

Magnetic monopoles

These are expected to be very massive, $m \sim 10^{16}$ GeV, with a magnetic charge $(e/\alpha) \approx 137$ e (according to Dirac quantization). They were once a stumbling block to grand unified theories because of the prediction of an extremely large density of these particles in the universe. The idea of inflation was brought to bear on the problem and the exponential expansion during this phase was shown to reduce their density to negligible levels. Figure 27 summarizes the upper bounds placed by various studies, carried out mostly deep underground, searching for a flux of these monopoles[33]. Even the bounds set by the experiments in the velocity domain around the expected $\beta \sim 10^{-3}$ are substantially below that implied by the closure density.

CHAMPS

The possibility that dark matter could consist of massive charged particles C^+, C^- with masses in the range 10–1000 TeV has been considered by Rujula *et al.* (ref. 34). These have been looked for using different techniques. Spiro[28] and colleagues at Saclay have made use of a method earlier adopted by P. Smith *et al.* of Oxford, noting that C would form hydrogenic atoms whose spectral lines would have a frequency approximately higher by a factor $[1 + (m_e/m_p)]$. Centrifugation of sea water concentrated any heavy atoms, and atomic spectroscopic techniques were used to look for a line due to $n=3 \rightarrow n=2$ transition; as shown in Figure 28, no line is seen, setting an upper bound of the concentration of $\sim 10^{-14}$, a hundred times smaller than that expected if these were to populate the halo at the requisite density. Barwick *et al.*[35] have searched for these particles in cosmic rays, and their upper bound rules out these particles as dark matter.

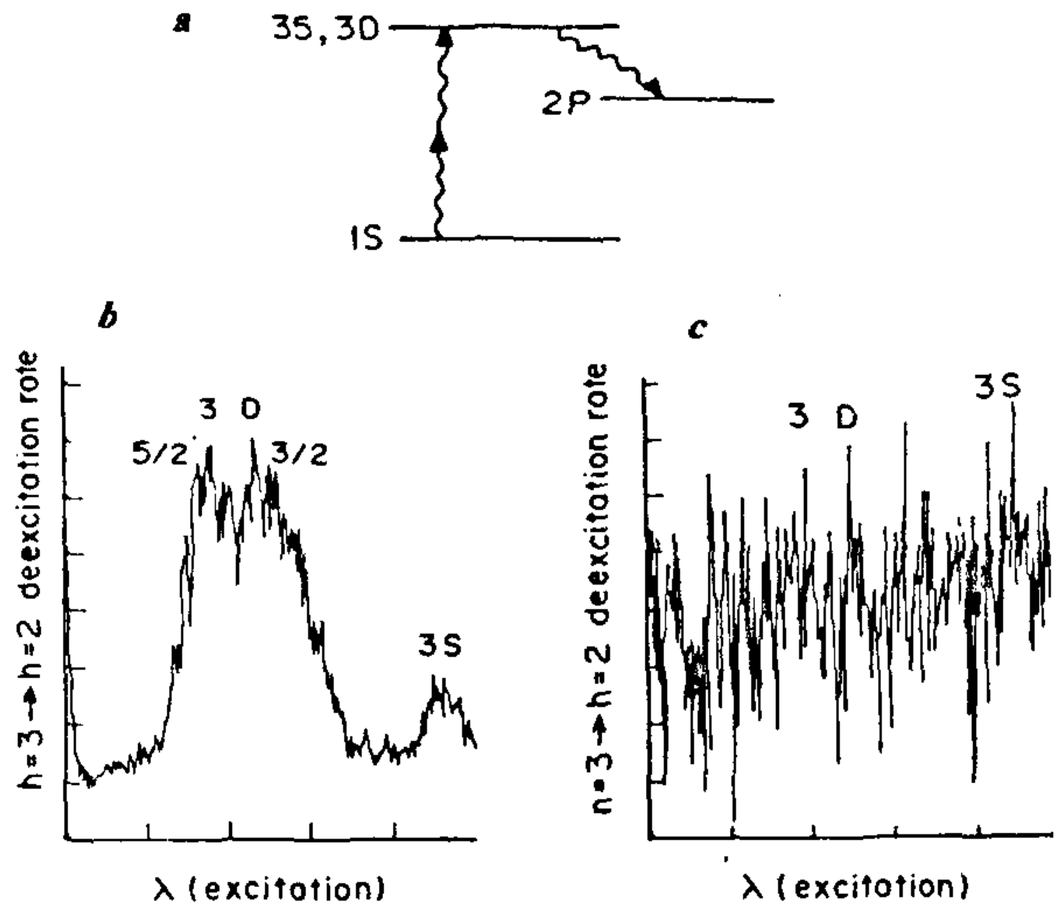

Figure 28. ***a***, The two-photon excitation to the 3S, 3D state of a hydrogenic CHAMP atom and its de-excitation to the P state. The left panel (***b***) shows clearly the de-excitation signal at the frequency expected for hydrogen but, as shown in the right panel (***c***) there are no transitions at the higher frequency corresponding to CHAMP atoms[28].

SIMPs

Strongly interacting massive particles (SIMPs) were first discussed by Sparkman. With mass in the range 10^6–10^8 GeV and with an interaction cross-section in the range $10^{-28} - 10^{-22}$ cm^2 have been ruled out by observations with silicon detectors operated specially to look for the high-energy deposition expected in the impact of such particles (see Figure 20).

Conclusion

Axions, neutralinos with a relatively narrow range of parameters, and the light neutrinos appear to be the most probable candidates for dark-matter particles. Attempts to directly measure axions with 1000 times higher sensitivity are under way. The search for neutralinos would require larger detectors with smaller backgrounds operated under very clean environmental conditions. In this context I show in Figure 29 the excellent shielding for the atmospheric muons that is obtained in the deep mines in Kolar Gold Fields, India —the induced radioactivity would also be correspondingly low. Finally, the light neutrinos, originally proposed as the first particulate candidate, still appear to be the simplest, if rather unexciting candidate.

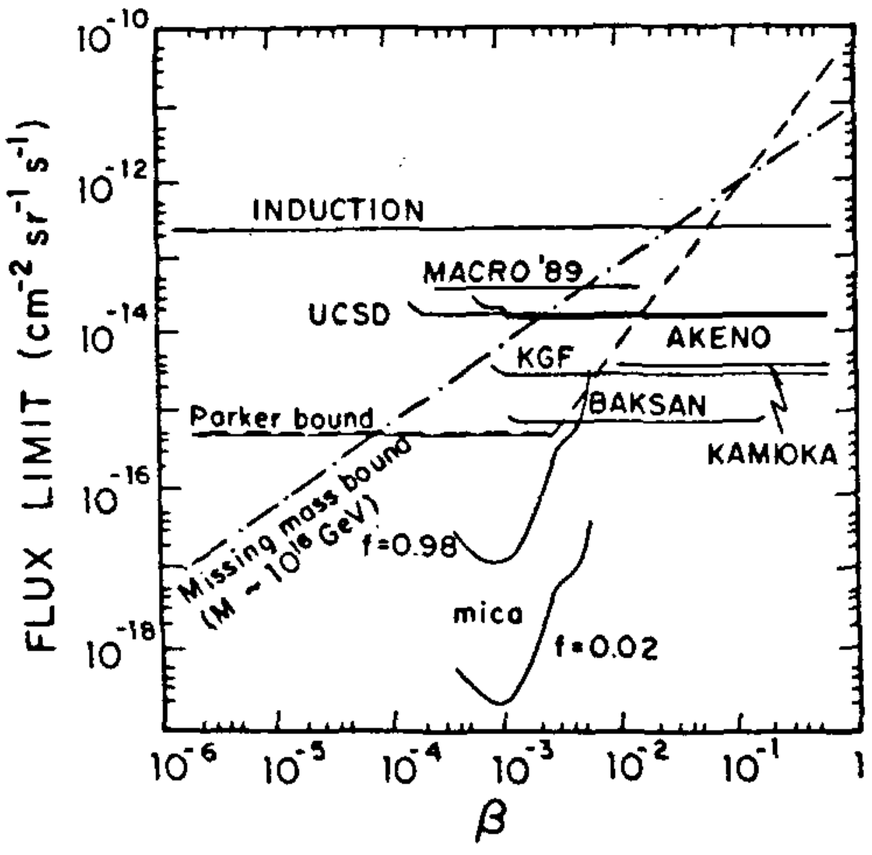

Figure 27. Bounds on the flux of magnetic monopoles established by various methods imply that they could not possibly be the constituents of dark matter.

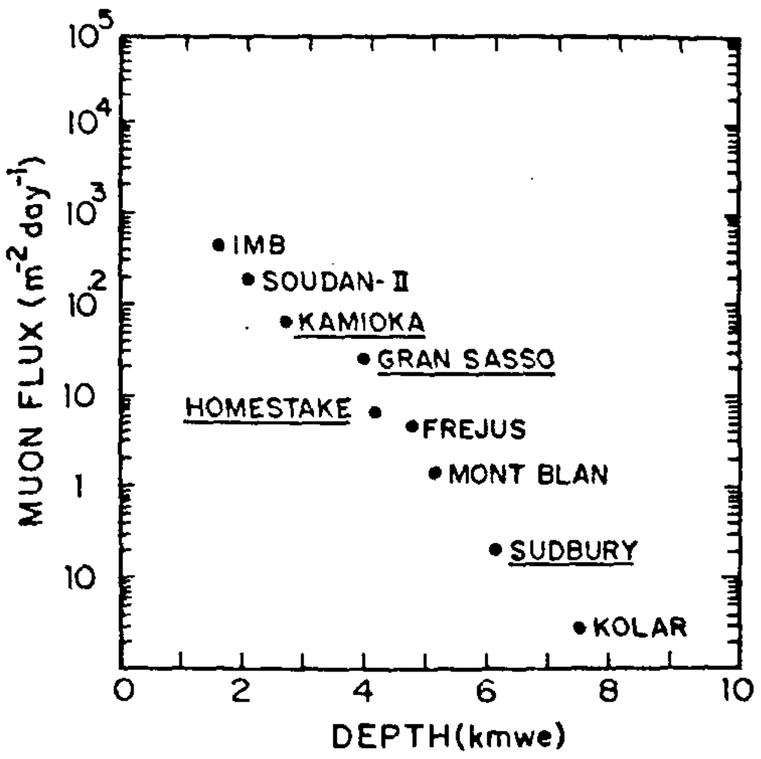

Figure 29. The excellent shielding to cosmic-ray muons achievable in deep mines shown as a function of depth in kilometre water equivalent.

Future detectors and search strategy

For dark-matter searches we need detectors of low background and high sensitivity to small-energy deposition. In view of this various kinds of cryogenic devices are being developed.

The germanium crystal

The success of the earlier studies has prompted the workers in the field to make these detectors sensitive also to the photons generated in the scattering process, which carries away typically 2 to 3 times as much energy as the ionization process. These are operated at temperatures of a few millidegrees Kelvin, where the Debye law indicates extremely low specific heats:

$$C \approx C_0 T^3. \tag{64}$$

Germanium thermistors measure the temperature pulse generated by thermalization of the phonons. Attempts are also under way to detect the ballistic phonons. If the phonon pulse is required to be in coincidence with the ionization pulse the backgrounds may be reduced dramatically.

The superheated superconductors

This device makes use of the superheating–supercooling phase transition exhibited by certain type-I superconductors. The material is kept in the form of tiny granules typically less than 0.1 mm in diameter. Whenever a scattering event takes place, depositing a small amount of energy, the granule makes a phase transition to the normal state. The magnetic flux change thus produced is measured.

Strategy

In the coming years the SUSY theories will be tested with improved sensitivity both at the LEP upgrade and also at the $\bar{p}p$ collider at Fermilab. This would fix the neutralino parameters more clearly, allowing us to perform and interpret experiments to search for these. Similarly the search for brown dwarfs should yield results soon, even though these cannot solve the full dark-matter problem. Finally we should not forget, in this excitement of the chase after new particles of high energy physics, the neutrinos, which we know definitely exist and populate the universe in sufficient numbers. We should continue with undiminished zeal experiments related to their mass, both direct ones and the indirect methods, for example by looking at their magnetic moment or with the solar neutrino deficits or with mixing and oscillations. For, in my view, and that of many others, it is here that we shall discover most clearly the physics beyond the standard model.

1. Zwicky, F., *Helv. Phys. Acta*, 1933, **6**, 110.
2. Rood, H. J., Page, T. L., Kinter, E. C. and King, I. R., *Astrophys. J.*, 1972, **172**, 627.
3. Cowsik, R. and McClelland, J., *Phys. Rev. Lett.*, 1972, **29**, 669.
4. Cowsik, R. and McClelland, J., *Astrophys. J.*, 1973, **180**, 7.
5. Faber, S. and Gallagher, J., *Annu. Rev. Astron. Astrophys.*, 1979, **17**, 135; Trimble, V., *Annu. Rev. Astron. Astrophys.*, 1987, **25**, 425; Kolb, E. W. and Turner, M. S., *The Early Universe*, Addison-Wesley, Redwood City, CA, USA, 1990; Biwsacy, J. and Tremaine, S., *Galactic Dynamics*, Princeton University Press, Princeton, 1987; Kormendy, J. and Knapp, G. (eds.), *Dark Matter in the Universe*, Reidel, Dordrecht, 1989; Turner, M. S., Fermilab preprint conference 91/78-A; Primack, J. R. and Seckel, D., *Annu. Rev. Nucl. Part. Sci.*, 1988, **38**, 751; Turner, M. S., Preprint no. Fermilab-Conf. 91/78-A, 1991; Caldwell, D., lectures given at the International School of Astroparticle Physics, Texas, 6 January 1991; Freese, K., a talk presented at the TEXAS/ESO-CERN Symposium, Brighton, UK, December 1990.
6. Boroson, T., *Astrophys. J., Suppl.*, 1981, **46**, 177.
7. Rubin, V. C., in *The Large Scale Characteristics of the Galaxy* (ed. Burton, W. B., IAU Symposium 84), Dordrecht, Reidel, 1979, p 211; *Astrophys. J.*, 1982, **261**, 439; in *Kinematics, Dynamics and Structure of the Milky Way* (ed. Shuter, W. L.), Dordrecht, Reidel, 1983a, p. 379; in *Internal Kinematics and Dynamics of Galaxies* (ed. Athanassoula, E., IAU Symposium 100), Dordrecht, Reidel, 1983b, p. 3; Rubin, V. C., Ford, W. K. Jr. and Thonnard, N., *Astrophys. J.*, 1980, **238**, 471; Rubin, V. C., Burstein, D., Ford, W. K. Jr. and Thonnard, N., *Astrophys. J.*, 1985, **289**, 81; Burstein, D., Rubin, V. C., Thonnarad, N. and Ford, W. R. Jr., *Astrophys. J.*, 1982, **253**, 70; Bosma, A., *Astrophys. J.*, 1981, **86**, 1825; Wevers, B. M. H. R., Ph D thesis, Groningen University, 1984; Einasto, J., *Teated Tartu Obs.*, 1970, **26**, 1; Ostriker, J. P. and Caldwell, J. A. R., in *The Large Scale Characteristics of the Galaxy* (ed. Burton, W. B, IAU Symposium 84), Dordrecht, Reidel, 1979, p. 441; Bahcall, J. N., Schmidt, M. and Soneira, R. M., *Astrophys. J. (Lett.)*, 1982, **258**, L23.
8. Cowsik, R. and Ghosh, P., *Astrophys. J.*, 1987, **317**, 26.
9. Loh, E. D. and Spiller, E. J., *Phys. Rev. Lett.*, 1986, **57**, 2865.
10. Oort, J. H., *Annu. Rev. Astron. Astrophys*, 1983, **21**, 373.
11. Bahcall, J. N., *Astrophys. J.*, 1984, **276**, 169.

12. Paczynski, B., *Astrophys. J.*, 1986, **304**, 1; De Rujula, A., Jetzer, Ph. and Masso, E., CERN preprint TH 5787/91 (and references therein).
13. Brandenberger, R., Kaiser, N., Schramm, D. and Turok, N., *Phys. Rev. Lett.*, 1987, **59**, 2371; Schramm, D. N. and Steigmann, G., *Astrophys. J.*, 1981, **243**, 1; Doroshkevich, A. G., *Sov. Astron.*, 1984, **28**, 378; Melot; M. L., Bond, J. R., Efstathiu, G. and Silk, J., *Phys. Rev. Lett.*, 1980, **45**, 1980; also see ref. 7 and references therein.
14. Lee, B. W. and Weinberg, S, *Phys. Rev. Lett.*, 1977, **39**, 165.
15. Ellis, J., Nanopoulos, D. V., Raizkowski, L. and Schramm, D. N., *Phys. Lett.*, 1990, **B245**, 252.
16. Turner, M. S., *Phys. Rep.*, 1990, **197**, 67; Raffelt, C. G., *Phys. Rep.*, 1990, **198**, 1.
17. ALEPH Collaboration, Decamp, D. *et al.*, *Phys. Lett.*, 1989, **B231**, 519; DELPHI Collaboration, Aarnio, P. *et al.*, *Phys. Lett.*, 1989, **B231**, 539; L3 Collaboration, Adeva, B. *et al.*, *Phys. Lett.*, 1989, **B231**, 509; OPAL Collaboration, Akrawy, M. Z. *et al.*, *Phys. Lett.*, 1989, **B231**, 530; MARK II Collaboration, Abrams, G. S. *et al.*, *Phys. Rev. Lett.*, 1989, **63**, 2173; ALEPH Collaboration, Decamp, D. *et al.*, *Z. Phys.*, 1990, **C48**, 365; DELPHI Collaboration, Abreu, P. *et al.*, preprint DELPHI 90–62 PHYS 80, contributed to the Aspen Conference, January 1991; L3 Collaboration, Adeva, B. *et al.*, L3 preprint no. 28, February 1991; OPAL Collaboration, Akrawy, M. Z. *et al.*, CERN PPE/91–67 (April 1991); Banerjee, S., Ganguli, S. N. and Gurtu, A., TIFR preprint EHEP–91–1; Banerjee, S., Talk at the Workshop on High Energy Physics Phenomenology II, Calcutta, January 1991, TIFR preprint EHEP–91–4; Krauss, L., *Phys. Rev. Lett.*, 1990, **64**, 999.
18. Dydak, F., rapporteur talk given at the 25th International Conference on High Energy Physics, CERN-PPE/11–14, Singapore, 1990; Ellis, J., Hagelin, J., Nanopoulos, D. V., Olive, K. A. and Sredniki, M., *Nucl. Phys.*, 1984, **B238**, 453.
19. Bowles, T. J., Proceedings of the 25th International Conference on High Energy Physics, Singapore, 1990; Holzschueh, E., Proceedings of the 14th International Conference on Neutrino Physics and Astrophysics, CERN, Geneva, 1990; Kawakami, H. *et al.*, in *Nuclear Weak Process and Nuclear Structure* (eds. Morita, M. *et al.*), World Scientific, Singapore, 1989; Lubimov, V. A. *et al.*, *Sov. Phys, JETP*, 1981, **54**, 616.
20. Caldwell, D. O., Eisberg, R. M., Grumm, D. M. Witherell, M. S., Sadoulet, B., Goulding, F. S. and Smith, A. R., *Phys. Rev. Lett.*, 1988, **61**, 510, and references therein.
21. Davis, R. *et al*, Proceedings of the 13th International Conference on Neutrino Physics and Astrophysics (ed. Schnepps, J. *et al*, Boston, 1988), World Scientific, Singapore, 1989, p. 518; Harata, K. S. *et al.*, *Phys. Rev. Lett.*, 1980, **63**, 16; see also Zatsepin, V. in these proceedings.
22. See Nakamura, K., rapporteuer paper 25th International Conference on High Energy Physics, Singapore, 1990, for an excellent review and full list of references.
23. Sciama, D. W., *Astrophys. J. (Lett.)*, 1991, **367**, L39.
24. Cowsik, R., *Phys. Rev. Lett.*, 1977, **39**, 784; *Phys. Rev.*, 1979, **D19**, 2219.; Gunn, J. E., Lee, B. W., Lerch, I., Schramm, D. N. and Steigman, G., *Astrophys. J.*, 1978, **223**, 1015; Falk, S. W. and Schramm, D. N., *Phys. Lett.*, 1978, **B79**, 511; Sarkar, S. and Cooper, A., *Phys. Lett.*, 1984, **B148**, 347; Dar, A. and Dado, S., *Phys. Rev. Lett.*, 1987, **59**, 2368; Rujula, de A. and Glashow, S. L., *Phys. Rev. Lett.*, 1980, **45**, 942; Shipman, H. L. and Cowsik, R., *Astrophys J.*, (*Lett.*), 1981, **247**, L111; Sato, K. and Terasava, N., *Phys. Lett.*, 1987, **B185**, 412; Dicub, D., Kolb, E. and Teplitz, R., *Phys. Rev. Lett.*, 1979, **39**, 169; Lindley, D., *Mon. Not. R. Astron. Soc.*, 1979, **188**, 15; Kolb, E. W. and Turner, Fermilab Pub-87/223-A, 1987.
25. Davidsen, A. F. *et al.*, *Nature*, 1991, **351**, 128.
26. Cowsik, R., *Indian J. Phys.*, 1981, **B55**, 497; Cowsik, R., *Challenges in Experimental Gravitation and Cosmology*, DST report, 1982; Cowsik, R., Tandon, S. N. and Krishnan, N., *Challenges in Experimental Gravitation and Cosmology*, DST *report*, 1982.
27. Smith, P. F. and Lewin, J. D., *Phys. Rep.*, 1990, **187**, 203.
28. Spiro, M., 'Detection of Dark Matter', talk given at Neutrino 1990, CERN, Geneva, 1990, and at the 25th International Conference on High Energy Physics, Singapore, 1990.
29. Stecker, F. W. and Tylkar, A., *Astrophys. J. (Lett.)*, 1989, **336**, 51.
30. Turner, M. S. and Wilczek, F., *Phys. Rev.*, 1990, **D42**, 1001, and references therein.
31. Kamionkowski, M., Fermilab preprint Conf. 91/61-A, 1991, and references therein.
32. De Panfilis, S. *et al.*, *Phys. Rev.*, 1989, **D40**, 3153; Hagmann, C., Sikivie, P., Sullivan, N. S. and Tarner, D. B., *Phys. Rev.*, 1990, **D42**, 1297, and references therein.
33. see ref. 20.
34. Rujula, A. de., Glashow, S. L. and Sarid, U., *Nucl. Phys.*, 1990, **B333**, 173.
35. Barwick, S. W., Price, P. B. and Snowden-ifft, *Phys. Rev. Lett.*, 1990, **64**, 2859.

Dedication. Professor Bernard Peters played a key role in the development of the Tata Institute of Fundamental Research; in grateful acknowledgement of the inspiration he has provided, I dedicate this article to him.